The unstable bridge from stimulus processing to correct responding in Parkinson's disease

Rolf Verleger [a,*], Henning Schroll [b,c,1], Fred H. Hamker [b,1]

[a] Department of Neurology, University of Lübeck, D 23538 Lübeck, Germany
[b] Department of Computer Science, Chemnitz University of Technology, Germany
[c] Bernstein Center for Computational Neuroscience, Charité University Medicine, Germany

*Corresponding author. Tel.: +49 451 5002916; fax: +49 451 5002489.
E-mail address: rolf.verleger@neuro.uni-luebeck.de (R. Verleger).

[1] HS and FHH contributed equally to this work.

keywords: action selection, basal ganglia, Parkinson's disease, P300, N_E, N-120

Abstract

It has been assumed that the basal ganglia implement links between stimulus (S) processing and motor response (R). It has also been proposed that the P3b component of the event-related EEG potential, which is usually as large in R- as in S-locked averages over trials, is a candidate marker to reveal integrity of S–R links. Therefore, the P3 complex (consisting of P3a and P3b) was here measured in averages over trials time-locked either to S or to the key-press R. P3b was expected to be equally large in healthy participants' R- and S-locked averages but to be smaller in R-locked than S-locked averages of patients with Parkinson's disease (PD) (n = 12 each), reflecting the loss of S–R links in PD.

It has been further assumed that the basal ganglia extract unambiguous results from complex signal patterns thereby resolving discrepancies between competing responses. If so, signals arriving at PD patients' cortex may still be discrepant and produce conflicts, as indicated by error-negativity (N_E)-type components even with PD patients' correct responses.

As expected, healthy persons had equal S- and R- locked P3b amplitudes and topographies, and PD patients had smaller P3b amplitudes in R-locked than S-locked averages. This latter result was due to an R-related fronto-central negative shift, overlapping PD patients' P3b in the final 100 ms before overt responding. This negativity might indicate response conflict even with correct responses. In line with this interpretation, PD patients had an N_E-type signal in error trials not only in R-locked averages, like healthy participants, but in S-locked averages as well.

These findings support the discrepancy-resolving hypothesis of the basal ganglia and suggest that the overlap of P3b by N_E-type components, related both to S and R, may reflect a major pathophysiological feature in Parkinson's disease.

1. Introduction

1.1. Basal ganglia and Parkinson's disease

Out of all brain structures, the basal ganglia are unique because they form a dense network of excitatory and inhibitory connections and largely depend on dopamine, a comparably slowly acting neurotransmitter (Rodriguez-Oroz et al., 2009). Well extending beyond the realm of motor functions (Brooks, 2006), the functional role of the basal ganglia may consist in implementing an information-routing system (e.g., Ashby, Ennis, & Spiering, 2007; Stocco, Lebiere, & Anderson, 2010; Schroll, Vitay, & Hamker, 2012), directing the transmission of signals between cortical regions, e.g., between some area engaged in perceptual processing like the visual cortex and some area engaged in movement control like the hand-motor cortex, thereby providing links for associating some response (R) to some stimulus (S). Stocco et al. (2010) more specifically proposed that, through a flexible routing mechanism, the basal ganglia provide automatic links between cortical regions, thereby reducing the number of necessary cortical computations (Fig. 1A).

An alternative proposal (Schroll, Vitay, & Hamker, in press) suggests that the basal ganglia are required not so much for maintaining automatic links between cortices but rather for acquiring these links, and that cortico-thalamo-cortical connections undertake control as links are automatized. The basal ganglia, however, remain essential for clearing discrepancies when competing S–R associations exist. More in detail, the model consists of a cortico-basalganglio-thalamic loop that contains four separate pathways, namely direct, indirect, and hyperdirect pathways of the basal ganglia (cf. Nambu, Tokuno, & Takada, 2002) and a cortico-thalamic pathway (cf. Haber, 2003). In contrast to previous computational models of cortico-basalganglio-thalamic loops (e.g., Brown, Bullock, & Grossberg, 2004; Frank, 2006;

Humphries, Stewart, & Gurney, 2006; Ashby et al., 2007; Stocco et al., 2010), pre-wiring of synaptic connections is minimized in Schroll et al.'s (in press) model. The model thus allows investigating synaptic self-organization within its different pathways, based upon the following core assumptions: synaptic plasticity in basal-ganglia pathways is modulated by dopamine which encodes error signals of reward prediction (cf. Hollerman & Schultz, 2003). High dopamine levels facilitate long-term potentiation (LTP) in direct and hyperdirect pathways and long-term depression (LTD) in the indirect pathway. Thereby, these basal-ganglia pathways learn to interlink S and R representations in such a way that correct responses are selected and reward delivery is maximized. Specifically, the direct pathway learns to link S representations to correct responses, while the hyperdirect pathway learns to suppress incorrect competing responses (Fig. 1B); during reversal learning, the indirect pathway learns to suppress previously correct responses, such that a new set of associations can be established afterwards. In contrast, synaptic plasticity in the cortico-thalamic pathway is not modulated by dopamine but is Hebbian-like (i.e., governed by pre- and postsynaptic activities only). Thus, rather than establishing S–R associations, the cortico-thalamic pathway slowly learns to automatize those S–R associations that have been previously interlinked by basal-ganglia pathways. It is shorter and thus faster than the route through the basal ganglia and establishes a synaptic memory of S–R associations that remains stable even if reward contingencies change. If the cortico-thalamic pathway connects some S to more than one R, basal ganglia remain vital even for well-trained S–R tasks. Otherwise, basal ganglia can be lesioned without task impairments.

Parkinson's disease (PD) is characterized by loss of dopamine-producing cells in the midbrain, depriving the basal ganglia of this relevant neurotransmitter (review

Rodriguez-Oroz et al., 2009). The above models imply that PD patients are impaired in making S-R connections (Stocco et al., 2010; Schroll et al., in press): The model by Stocco et al. (2010) suggests that the automatic routing from S to R through the basal ganglia is impaired in PD while cortico-cortical connections might continue to interlink S and R. Consequently, basal ganglia impairment will result in increased cortical processing (Fig. 1A). Schroll et al.'s (in press) model predicts that when dopamine neurons are lesioned, the direct pathway unlearns to interlink stimuli and correct responses. Moreover, the indirect pathway learns to detrimentally inhibit correct responses and the cortico-thalamic pathway learns to detrimentally facilitate incorrect responses (Fig. 1B). Thus, the links between stimuli and correct responses become unreliable and response conflicts arise which might be particularly strong when stimuli simultaneously trigger several responses.

The impairments suggested by the above models are not necessarily seen in overt behavior because continuing cortico-cortical (Stocco et al., 2010) or cortico-thalamo-cortical connections (Schroll et al., in press) may at least partly maintain the links from S to R. Thereby, the correct R, although less strongly facilitated, might still receive enough basal-ganglia activation to become the dominant one. Yet this divergence of PD patients from healthy functioning might be reflected in neurophysiological measures.

1.2. ERPs and basal-ganglia dysfunction

Event-related EEG potentials (ERPs) recorded at the scalp reflect neuronal processing in the cerebral cortex. Activity of the basal ganglia cannot be directly measured, due to their distance from the scalp (Lutzenberger, Elbert, & Rockstroh, 1987) and because their anatomy and physiology does not allow for the parallel mass

activity of compensatory flow of charge near the dendrites that constitutes the basis for scalp-recorded EEG (Birbaumer, Elbert, Canavan, & Rockstroh, 1990). Thus, what may be expected to be measured in PD patients' ERPs is not any dysfunctional activity of the very basal ganglia but rather those changes in cortical activity that are either directly due to, or needed to compensate for, the hypothesized dysfunctions (review: Verleger, 2012). The present study focuses on the P3b and on N_E-type components of the ERP, measuring these components both in their customary way, relating P3b to S and N_E to R, as well as in an unconventional way, relating P3b to R and N_E to S.

1.3. The P3b component and basal-ganglia dysfunction

From studies in healthy participants, there is reason to believe that the ERP component most closely related to the link between S processing and R organization is the P3b, i.e., the parietally focused part of the P300 complex, overlapping and following the fronto-central ‘P3a' part (Squires, Squires, & Hillyard, 1975; reviews: Verleger, 1988; Polich, 2007). The mediating role of P3b may be inferred from the dual-sided relation of its single-trial variability both to S and to R. This dual-sided relation has been demonstrated by mathematical modeling (Gerson, Parra, & Sajda, 2005; Takeda, Sato, Yamanaka, Nozaki, & Yamamoto, 2010; Ouyang, Herzmann, Zhou, & Sommer, 2011; Ouyang, Schacht, Zhou, & Sommer, 2013), by analysis of intracranial recordings (with their good signal/noise ratio; Roman, Brázdil, Jurák, Rektor, & Kukleta, 2005), by the unique relation of P3b latency to the time-point of decision (O'Connell, Dockree, & Kelly, 2012) and by P3b amplitude's sensitivity to repeating a decision (Race, Badre, & Wagner, 2010). Importantly, because also used in the present study, amplitudes of P3b have been compared between the usual “S-

locked" averages, where single trials are aligned for averaging at their time-points of S onset, and "R-locked" averages, where single trials are aligned for averaging at the time-points of the key-press R (made in response to S). In young healthy participants, P3b has been found to be equally large in S- and R-locked averages (Poli, Cinel, Citi, & Sepulveda, 2010; Verleger, Jaśkowski, & Wascher, 2005; Saville et al., 2011).

The P3b component has been recorded from patients with PD in a number of studies, generally in go/no-go or choice-response tasks. Results were inconsistent. When evoked by visual stimuli (as will be used in this study) P3b amplitudes were smaller in PD patients than in healthy controls in a few studies (Beste, Dziobek, Hielscher, Willemssen, & Falkenstein, 2009; Pulvermüller et al., 1996), frequently of equal size in both groups (Bokura, Yamaguchi, & Kobayashi, 2005; Low, Miller, & Vierck, 2002; Praamstra, Meyer, Cools, Horstink, & Stegeman, 1996; Praamstra, Stegeman, Cools, & Horstink, 1998; Stemmer, Segalowitz, Dywan, Panisset, & Melmed, 2007; Tachibana, Toda, & Sugita, 1992; Tachibana, Aragane, Kawabata, & Sugita, 1997; Willemssen, Falkenstein, Schwarz, Müller, & Beste, 2011; Wright, Geffen, & Geffen, 1993) or even larger in patients with PD (Fogelson, Fernandez-del-Olmo, & Santos-Garcia, 2011; Schmiedt-Fehr, Schwendemann, Herrmann, & Başar-Eroğlu, 2007).

All those studies measured P3b in S-locked averages. In the present study, P3b components were measured both in S-locked and in R-locked averages. If indeed P3b reflects the bridge between S and R and if the basal ganglia play a role for building this bridge, then PD patients' P3b might differ from healthy participants': It might only be in healthy participants that S-locked and R-locked P3 are equally large whereas, by not linking the S-triggered processing to R in a regular fashion any more,

PD patients' P3b might not be time-locked with R, and so R-locked P3 should be smaller than S-locked P3.

1.4. The N2 and N_E family of components and basal-ganglia dysfunction

Schroll et al. (in press) assumed that, in well-practiced tasks, the basal ganglia are required to reduce S-R conflicts (if existent) by favoring the desired response via the direct pathway and inhibiting undesired responses via the hyperdirect pathway. Based on this assumption, it makes sense to look at ERP markers of conflict. Several negative components have been reported to be such markers. We will describe here the ones that are relevant to the present task, to outline a framework for the negative component that occurred in our data. Yeung, Botvinick, and Cohen (2004) highlighted the anterior N2b and the N_E. N2b, measured in S-locked averages of correctly responded trials at 200–350 ms after stimulus onset, indicates that S or R deviate from the standard S or R in a given task, reflecting response conflict (Kopp, Rist, & Mattler, 1996) and requiring cognitive control (Folstein & van Petten, 2008). N_E, the "error negativity" (Falkenstein, Hohnsbein, Hoormann, & Blanke, 1991), measured in R-locked averages of incorrectly responded trials immediately after execution of the incorrect R, likewise indicates response conflict, requiring cognitive control (Yeung et al., 2004). It is most probably generated in the medial frontal cortex, probably including the anterior cingulate cortex (Ridderinkhof, Ullsperger, Crone, & Nieuwenhuis, 2004; Debener et al., 2005). There is some evidence that N2b and N_E reflect similar processes and may be generated in the same cortical areas (Yeung et al., 2004; Cavanagh, Zambrano-Vazquez, & Allen, 2012). But they are not the same, because N2b occurs in correct trials (though after conflict-inducing stimuli)

and N_E in incorrect ones, and N2b occurs around 300 ms after S onset, which might be well before R, whereas N_E occurs not earlier than R.

Two other components need mentioning, N_C and N-120. As just described, N_E is measured in incorrect trials immediately after R in R-locked averages. It is usually compared to the corresponding epoch, immediately after R in R-locked averages, of correct trials. But it has been noticed that this epoch in correct trials may contain some negativity as well, "N_C", though much smaller than N_E (Vidal, Burle, Bonnet, Grapperon, & Hasbroucq, 2003). Like N_E, N_C has been linked to cognitive control (Vidal et al., 2003) but there may simply be some contributions from sensorimotor reafference (Yordanova, Falkenstein, Hohnsbein, & Kolev, 2004). Recently, another R-locked negativity has been described, preceding the correct response in high-conflict trials by about 120 ms (Mansfield, van der Molen, & van Boxtel, 2012; Vidal, Burle, Grapperon, & Hasbroucq, 2011) rather than following R, as does N_C. It may be suspected that, by its occurring before R, this "N-120" is N2b, only measured in the R-locked average rather than in the S-locked average, but actually the two components, N2b and N-120, could be differentiated in both studies (Mansfield et al., 2012; Vidal et al., 2011).

N2b, N_E, and N_C have been measured in patients with PD. Like results on P3b, results on N2b recorded in tasks with visual stimuli have been inconsistent. Often, N2b amplitudes were smaller in PD patients (Bokura et al., 2005; Fogelson et al., 2011; Praamstra & Plat, 2001) but there is also evidence to the contrary (Beste et al., 2009; Willemssen et al., 2011). Results on N_E in PD have met with particular interest because an influential assumption suggested that N_E is fed by dopamine-mediated signals from the basal ganglia, in line with the well-documented functions of the basal ganglia in reinforcement-learning, and, therefore, that N_E should be reduced in PD

(Holroyd & Coles, 2002). Indeed, several studies found N_E reduced in PD (Falkenstein et al. 2001; Ito & Kitagawa, 2006; Stemmer et al., 2007; Willemssen, Müller, Schwarz, Hohnsbein, & Falkenstein, 2008; Willemssen, Müller, Schwarz, Falkenstein, & Beste, 2009) whereas Holroyd, Praamstra, Plat, and Coles (2002) could not verify their prediction. Based on the discrepancy-clearing model by Schroll et al. (in press) and the notion of conflicting response tendencies, another prediction on the N2b-N_E family may be made: conflicting signals may remain unresolved in PD due to basal-ganglia dysfunction and will, therefore, reach the cortex even when overt responses are correct. The presence of such conflicting signals might evoke an N_E-type component in PD with correct responses as well, either before R (cf. the above-noted N-120) or, at least, immediately after R. Indeed, an increased N_C, immediately after R, has been reported in newly diagnosed PD patients (Willemssen et al., 2009) but not in the other studies that reported N_C measures in PD (Ito & Kitagawa, 2006; Willemssen et al., 2008). According to our knowledge, no study has looked so far for an N-120-type component in PD, i.e., for an indicator of response conflict immediately before R.

We reasoned that abnormalities of PD patients' P3b and N_E/N2b-type components might affect and cancel each other due to the opposite polarity of these components. To disentangle such possible interactions, we measured N_E not only in R-locked averages as usual, but also in S-locked averages. There are only very few studies that compared N_E between R-locked and S-locked averages of error trials (Maier, di Pellegrino, & Steinhauser, 2012) and we are not aware of any such studies on patients with PD. Thus, S- and R-locked averages were compared to each other both in correct-response trials (cf. above, Section 1.3) and in error trials.

1.5. Summary of hypotheses

(1) While S-locked P3 is not expected to differ between groups, there will be a difference between groups in the relation between R-locked and S-locked P3b (i.e., the parietal part of P3):

(1.a) S-locked and R-locked P3b will be equally large in healthy participants.

(1.b) In contrast, R-locked P3b will be smaller than S-locked P3b in PD. This prediction is in line with both Stocco et al.'s (2010) and Schroll et al.'s (in press) model which both predict losses in the processing chain from S to R in PD patients, resulting in less consistent activation of R.

(2) A conflict-related negative component similar to N_E will occur in PD patients' correctly responded trials, possibly immediately before R. This hypothesis is in line with Schroll et al.'s (in press) model which predicts increased cortical response conflict in PD patients.

The two irregular features of PD patients outlined in hypotheses (1.b) and (2) might overlap and, therefore, will have to be disentangled by systematically comparing S- and R-locked averages in correctly and incorrectly responded trials.

To pursue these questions, data obtained in a flanker task (Verleger et al., 2010) were reanalyzed. This task has been used several times for recording ERPs from PD patients. What has never been done before with PD patients' data, neither from a flanker task nor from any other task, is comparing the usual S-locked P3 to R-locked P3 and consequently drawing the link between features of PD patients' N_E to specific features of their P3b.

2. Material and methods

2.1. Participants

All participants took part after having given written informed consent. The study was approved by the local Ethics Committee. Most participants were right-handed, as evaluated by the Edinburgh Handedness Inventory (Oldfield, 1971), except one ambidextrous control participant (PD patients: mean 83, range 33–100; control group: mean 69, range 9–100; $t(22) = 0.2$, n.s., for differences between groups). Short-sighted participants wore their glasses throughout the experiment.

2.1.1. PD patients (n=12)

These were patients attending our outpatient clinic. Of the initial 14 participants, one was excluded for possible dementia and one for failure to follow task instructions. Individual data of the remaining 12 patients are compiled in Table 1. They were 9 men and 3 women, mean age 65 years (range 50–79 yr). Average disease duration was 4 years (1–12 yr), scores on the modified Hoehn–Yahr scale (Goetz et al., 2004) were 2.1 on average, ranging between 1 (one patient) and 3 (two patients), and UPDRS III scores (Fahn, Elton, and members of the UPDRS development committee, 1987) ranged between 5 and 40, mean 19.3 (78.4). All patients received dopaminergic medication, with an average L-dopa equivalence dose of 520 mg (7320 mg; range 150–1050 mg) and were tested at their best clinical “on”. None of them had a positive family history of PD.

2.1.2. Healthy controls (n=12)

Of the initial 14 participants, one had to be excluded because of failure to follow task instructions and one due to too many artifacts in her EEG. Participants

included 4 men and 8 women, many of them PD patients' spouses, mean age 68 years (range 55–75 yr). None suffered from any illness affecting the central nervous system, and each one had a Hoehn–Yahr score (Goetz et al., 2004) of 0. UPDRS III scores (Fahn et al., 1987) were 0 in seven participants and ranged from 1 to 4 (median 2) in the five other participants.

2.2. Stimuli

A flanker task was used (as in many of the studies on PD mentioned in Sections 1.3 and 1.4). Stimuli appeared in black at a distance of 1.2 m from participants' eyes on the white background of a 17″ screen (1024 x 768 pixels) which was driven at 75 Hz. Stimuli are depicted in Fig. 2. The target stimulus was an arrow pointing left or right. The arrow consisted of two parallel open triangles, each 1.0° high and 0.45° wide, spaced 0.1° apart. Thus, the arrow was 1.0° wide (2 x 0.45°+0.1°). The target was flanked by other arrows that had to be ignored, one on the left and one on the right, with their innermost points 0.7° off center, 0.2° from the outermost points of the target. A small red fixation cross (0.1° x 0.1° was always visible. Targets were presented in the center of the screen for 107 ms, and the two flankers were simultaneously presented left and right off center for 13 ms. The flanker–target interval ("FTI"; flanker offset to target onset) was either 0 ms or 107 ms (called FTI 0 and FTI 100 in the following, for simplicity) combining the two intervals most often used in previous studies. The two intervals were changed in random order across trials.

The flanker arrows pointed to the same direction in a given trial, either left or right. Independently, the central target arrow pointed left or right, either compatible or incompatible with the flankers. In 50% of trials, flankers were immediately followed

at their locations for 107 ms by a masking pattern of overlapping left and right arrow stimuli (cf. Seiss & Praamstra, 2004). These masked-flanker trials will here serve as neutral comparison for the trials with unmasked compatible or incompatible flankers.

2.3. Procedure

Participants were seated in a comfortable armchair in a darkened room in front of the computer screen and held a computer keyboard on their lap. Presentation® software (www.neurobs.com) was used to present the stimuli, record responses, and send stimulus and response codes to the computer that recorded EEG.

Participants had to press the lower left or right key (left ctrl and numpad-enter) according to arrow direction which changed across the 640 trials in random order. Flanker–target relations also changed in random order: there were 80 compatible, 80 incompatible, and 160 neutral-flanker trials with FTI 0 and FTI 100 each. The next trial started 1.5 s after the key-press response.

2.4. EEG recording and processing

EEG was recorded with Ag/AgCl electrodes affixed in an EEG cap according to the 10–20 system (FMS, Munich) from 3 midline sites (Fz, Cz, Pz), 16 lateral sites, and the nose-tip. On-line reference was Fz, ground was FCz, data were off-line re-referenced to the nose-tip. For artifact control, vertical EOG was recorded from above vs. below the right eye and horizontal EOG from positions next to the outer rims of the eyes. Data were amplified within 0–1000 Hz by a BrainAmp MR plus and stored at 250 Hz per channel. Off-line, data were low-pass filtered at 30 Hz, and segmented from 200 ms before target onset to 1100 ms afterwards. Editing trials for artifacts included rejecting trials when voltages in the EEG exceeded 7100 mV or when

consecutive data points differed by more than 50 mV, then correcting ocular artifacts using the linear regression method implemented in the BrainAnalyzer software, and thereafter rejecting trials when voltages exceeded 775 mV or the negative and positive maximum differed by more than 100 mV. Data were referred to baseline 200–100 ms before target onset (to be before flanker onset also in FTI 100 trials). To obtain ERPs, data were averaged across artifact-free trials with key-press responses within 200–1000 ms after target onset, separately for each condition and participant, pooled across trials with left and right responses. This was done for correctly responded trials in all conditions, and additionally for incorrectly responded incompatible FTI 100 trials, where most errors occurred. Averaging was done both in the S-locked way, aligning the segments across trials at target onset, spanning 200 ms before to 1100 ms after target onset, and in the R-locked way, aligning segments across trials at response onset, spanning 400 ms before to 100 ms after response onset for measuring P3 and spanning 300 ms before to 200 ms after response onset for measuring N_E. Note that the choice of these window boundaries for S- and R-locked trials, together with the response- time limits of 200–1000 ms guarantees that the same number of trials will be included in the S- and R-locked averages. This was verified for each participant. For correctly responded trials, the minimum number of included trials was 35, with a mean number of 67 for conditions with visible flankers and of 134 for conditions with neutral (masked) flankers. For error trials in the incompatible FTI 100 condition, the minimum number of trials per included participant was 3. Three participants of either group did not fulfill this criterion. The median number of trials was 6 (range 3–16) for the included nine control participants and 11 (range 5–28) for the included nine PD patients.

2.5. Quantification and statistical analyses of task performance and of ERPs

A global analysis of participants' behavior and analyses of S-locked lateralized readiness potentials (recorded at lateral sites above the motor cortex) have been reported in Verleger et al. (2010). The P3 and N_E-type components which will be analyzed in the present report had remained unmentioned in that paper.

To characterize task performance in detail, correctness and speed of responses were assessed. The first four trials were discarded, allowing participants to reach steady-state performance. In order to have unambiguous responses, data were screened for occasional double key-press responses. In case of double presses of the correct key, the first key-press was taken as response time (RT). Correct–incorrect responses were removed from analysis. Incorrect-correct and incorrect-incorrect responses were counted as errors. Error percentages were determined as numbers of incorrect and missing (>1000 ms) responses relative to all responses. These error rates were arcsin-transformed, to approach normal distribution. RTs were measured relative to target onset and will be reported for trials only that entered EEG analysis, i.e., trials that did not only satisfy the response criteria but also were free of EEG artifacts. Means and intraindividual standard deviations (SD) of these RTs were calculated for each condition.

For graphical comparison of ERPs (Figs. 4, 5, 8), S- and R-locked grand means were first overlaid such that time-point zero of the R-locked averages (the time-point of responding) coincided with the mean response time (RT) in S-locked averages (which was, e.g., in Fig. 4, 560 ms). But when doing so, the R-locked waveforms systematically lagged behind the S-locked waveforms by about 50 ms. In our previous paper that compared S- and R-locked averages (Verleger et al., 2005) responses were measured by force-sensitive keys, producing continuous force-

waveforms. On these force waveforms, the time-point of optimum overlap of S- and R-locked averages could be freely chosen and was then fixed at a response force of 2 N. Lacking this possibility in the present study, where usual all-or-none keys were used, we chose the pragmatic solution of shifting the R-locked waveforms backward by 48 ms (such that, e.g., in Fig. 4, R-locked time-point zero was at S-locked 512 ms rather than 560 ms). Note that this backward shift was done to enable easy eye-ball comparison between S- and R-locked grand means and did not affect the actual measurements taken separately in the S- and R-locked waveforms.

After inspecting the grand means of correctly responded trials, latency windows for the P3 complex were defined as 250–700 ms after target onset in the S-locked averages and 300 ms before to 80 ms after response onset in the R- locked averages. P3 was measured as largest positive peak in the three midline channels Fz, Cz, Pz.

N_E was measured in R-locked averages of error trials of the incompatible FTI 100 condition. It was defined as largest negative peak 0–150 ms after R onset. Its amplitude was measured with reference to the preceding positive peak (as commonly done, e.g., Falkenstein et al., 2001; Stemmer et al., 2007) 0–150 ms before R onset. Peak latencies were determined at Cz, and amplitudes were measured at Fz, Cz, Pz at these latencies. In a second analysis, this R-locked N_E from error trials was compared to correct-response data. Since there was no distinct peak in many participants' correct-response data 0–150 ms after R onset, amplitudes were computed as means of 50ms time epochs. Third, N_E was compared to its S-locked equivalent by comparing the 50 ms epochs of maximum amplitude: 50–98 ms after R onset for R-locked N_E vs. 372–420 ms after S onset for its S-locked equivalent. Fourth, the S-locked N_E equivalent was compared to the same time-period during correctly responded trials. In

order not to miss relevant differences, a broad time-span of six 50 ms epochs was covered, 200-500 ms after S onset.

Analyses of variance (ANOVAs) were used for statistical analyses. The factors will be described in the Results section. To interpret interactions, ANOVAs were conducted separately for the levels of each of the interacting factors. Degrees of freedom of repeated-measurement factors with more than two levels were corrected by means of the Greenhouse–Geisser method.

3. Results

3.1. Error rates and response times

Responses were slower than 1 s in 2% of trials, and correct-incorrect double responses occurred in less than 1% of trials, without differences between PD patients and control group ($F_{1,22}$ and $F_{2,44} < 1.8$, n.s.). In the remaining trials, arcsin-transformed error rates, mean RTs, and intraindividual SD of RTs were analyzed by ANOVAs with the between-subjects factor Group (PD, healthy) and the repeated-measurement factors Flanker Type (compatible, neutral, incompatible) and Flanker–Target–Interval (FTI; 0 ms vs. 100 ms interval between flankers and target).

Responses were correct in 97% of trials, except with incompatible flankers at FTI 100 (PD patients: 84%; control group: 90%). This increased error rate in FTI 100 was reflected in main effects of FTI and of Flanker Type and in an interaction of FTI x Flanker Type, all $F_{1,22}$ and $F_{2,44} > 21.0$, all $p < 0.001$. This effect being more distinct in PD patients was reflected in a marginally significant interaction of FTI x Group, $F_{1,22} = 4.1$, $p = 0.054$ (cf. Wylie et al., 2009, for similar effects).

Mean RTs of the correctly responded trials (connected values in top panel of Fig. 3) were faster with compatible than incompatible flankers, $F_{2,44} = 138.2$, $p <$

0.001, more so with FTI 100 than with FTI 0 (FTI x Flanker Type $F_{2,44} = 93.9$, $p < 0.001$). Effects of flanker type did not differ between patients and control group (unlike, e.g., in Praamstra et al., 1998), all effects of Group $F_{1,22}$ and $F_{2,44} < 0.8$.[2] Besides, mean RTs were faster with FTI 100 than FTI 0 (FTI: $F_{1,22} = 17.4$, $p < 0.001$).

The groups did not differ in variability of RTs, as measured by SDs over correct trials (connected values in bottom panel of Fig. 3), all effects of Group yielding $F_{1,22}$ and $F_{2,44} < 1.5$. RTs varied more with FTI 100 than with FTI 0, $F_{1,22} = 10.7$, $p = 0.003$.

RTs in error trials with incompatible flankers at FTI 100 were analyzed in nine participants of either group who had at least three error trials free of EEG artifacts (rightmost values in Fig. 3). There were no significant effects of Group on mean and variability of error RTs, $t_{16} < 0.9$, n.s. Wrong responses were much faster than correct ones (372 ms vs. 592 ms, $F_{1,16} = 308.3$, $p < 0.001$). RT variability varied widely across participants (Fig. 3) with some participants committing their errors with nearly fixed fast RTs and others committing both fast and slow errors.

3.2. Correct-response ERPs

ANOVAs were conducted on amplitudes and latencies of P3, including the factors Group, Flanker Type, and FTI, as above (Section 3.1), and additionally the two repeated-measurement factors Reference Event (S-locked vs. R-locked) and Recording Site (Fz, Cz, Pz).

---

[2] When masked flankers were separated into compatible and incompatible flankers, there was a small but reliable effect of masked-flanker type on PD patients' responses: Their RTs were 13 ms faster with masked compatible than incompatible flankers, which was not the case in the healthy controls, Masked- Flanker Type–Group $F(1,23) = 4.9$, $p = .04$. This replicates Seiss and Praamstra's (2004, 2006) findings of larger response activation induced by masked flankers in PD patients than in healthy controls.

Fig. 4 shows the major result of this study: R-locked P3 from the three midline sites was smaller than S-locked P3 in PD patients, whereas these two measurements of P3 did not differ in the control group: Reference Event $F_{1,22} = 7.74$, $p = 0.01$; Reference Event x Group $F_{1,22} = 7.72$, $p = 0.01$; effect of Reference Event in PD patients $F_{1,11} = 23.3$, $p < 0.001$; in the control group $F_{1,11} = 0.0$, n.s. This result is in agreement with hypothesis 1.a (equal S- and R-locked P3b in the control group) and hypothesis 1.b (reduced R-locked P3 in PD patients).

This effect of Reference Event x Group was qualified by its interaction with Recording Site, $F_{2,22} = 3.5$, $p = 0.047$. Separate ANOVAs at each recording site in either group showed that, as suggested by Fig. 4, the PD patients' reduction of R-locked P3 was not largest at Pz, as expected by hypothesis 1.b, but rather at Cz: effect of Reference Event in the PD patients at Fz: $F_{1,11} = 7.9$, $p = 0.02$; at Cz: $F_{1,11} = 57.3$, $p < 0.001$; at Pz: $F_{1,11} = 3.3$, $p = 0.10$. In the control group, R-locked P3 was also smaller than S-locked P3 at Fz, $F_{1,11} = 9.9$, $p = 0.009$, but R- and S-locked P3 did not differ from each other at Cz and Pz, $F_{1,11} < 1.3$, n.s. These topographical relations are best seen in scalp maps of the R- minus S-locked differences, displayed in the top row of Fig. 5.

The Reference Event x Group effect, reflecting PD patients' reduction of R-locked P3, was not modified by Flanker Type and FTI (all F-values < 1.8, all $p > 0.17$), thus principally held across all six combinations of Flanker Type FTI, with their widely varying range of RTs. This reproducibility of the effect in the single combinations is illustrated by Fig. 6.

Independently of groups and reference events, P3 was smaller at Fz than at Pz and Cz (main effect of Recording Site $F_{2,22} = 14.7$, $p < 0.001$). Amplitudes tended to be larger at Pz than at Cz throughout, except for the condition with incompatible

flankers at FTI 100 (Recording Site x Flanker Type $F_{4,44} = 2.8$, $p = 0.048$; Recording Site x Flanker Type x FTI $F_{4,44} = 3.7$, $p = 0.01$).

Since PD patients' reduction of R-locked P3b was largest at Cz, where neither P3a nor P3b are most distinct, the reduction apparently was not due to response-related latency variation of the P3b components but due to overlap of some additional, response-related negative process. By applying S- and R-locked averaging to incorrectly responded trials, we explored whether this negative process in correct trials has some relationship to the error negativity N_E, which is measured in incorrect trials.

3.3. Incorrect-response ERPs

R-locked grand means across incorrectly vs. correctly responded trials with incompatible flankers at FTI 100 are shown in Fig. 7 from the nine participants per group with at least three artifact-free error trials. The error-negativity N_E is clearly seen in both groups. Error minus correct difference maps are displayed in Fig. 5. In an ANOVA with the factors Group and Recording Site, N_E amplitude (measured against the preceding positive peak) did not differ between groups, $F_{1,16} = 0.3$, n.s. ($F_{1,16} = 1.4$, $p = 0.25$, in ANOVA on Cz data only) although Cz amplitudes were larger on average in the control group (-11.5 mV ± 3.8 mV SD) than in the patients (-9.2 mV ± 4.6 mV SD). Mean N_E latency was 74 ms (±29 ms SD) without difference between groups, $F_{1,16} = 0.1$, n.s. Nor was a group difference obtained in an ANOVA on three 50 ms epochs, from 0 ms to 150 ms after R (ANOVA factors being Group and Recording Site again, additionally Correctness, i.e., wrong vs. right, and Epoch): A main effect of Correctness indicated the reliable occurrence of N_E ($F_{1,16} = 14.2$, $p = 0.002$), largest in the 50–98 ms epoch (Correctness x Epoch: $F_{2,32} = 5.2$, $p = 0.02$) and

more marked at Cz and Pz than at Fz (Correctness x Recording Site: $F_{2,32} = 3.6$, $p = 0.04$) but Interactions of Correctness with Group were not significant, $F <= 1.4$, $p >= 0.26$.

These R-locked data from error trials are overlaid with S-locked data from the same trials in Fig. 8, as was done above (Fig. 4) for correct-response trials. R- minus S-locked difference maps are displayed in Fig. 5. N_E appears evident in the S-locked data of Fig. 8, more so in PD than in the control group. However, when the R-locked 50 ms epoch where N_E was largest (50–98 ms after R) was compared to the corresponding S-locked 50 ms epoch (372– 420 ms after S) in an ANOVA with the factors Group and Recording Site (as before) and Reference Event (R vs. S), N_E was larger in R-locked than in S-locked data ($F_{1,16} = 6.4$, $p = 0.02$) without any difference between groups ($F < 0.8$, n.s., for Reference Event x Group and Reference Event x Group x Recording Site).

Differences between the two groups became more obvious when comparing error trials to correct-response trials in S-locked data (Fig. 9). An ANOVA on six epochs ranging from 202 ms to 500 ms after S, with the factors Group, Recording Site, Correctness, and Epoch, yielded effects of Correctness x Group (tendency: $F_{1,16} = 4.2$, $p = 0.056$), Correctness x Epoch x Group ($F_{5,80} = 3.2$, $p = 0.046$), and Correctness x Epoch x Recording Site x Group ($F_{10,160} = 2.9$, $p = 0.02$). To resolve these interactions, effects of Correctness x Group and Correctness x Recording Site x Group were tested in each epoch separately. These effects were significant at 252–300 ms ($F_{1,16} = 5.9$, $p = 0.03$ and $F_{2,32} = 4.6$, $p = 0.03$) due to a tendency for larger positivity in error than correct trials in the control group (Correctness: $F_{1,8} = 4.2$, $p = 0.08$; Correctness x Recording Site: $F_{2,16} = 3.4$, $p = 0.09$) versus no effect in PD ($F < 2.2$) and were significant at 352–400 ms ($F_{1,16} = 5.5$, $p = 0.03$ and $F_{2,32} = 4.6$, $p =$

0.02) due to larger negativity in error than correct trials in PD (Correctness: $F_{1,8} = 8.5$, $p = 0.02$) with the largest effect at Pz and the smallest, but still significant effect at Fz (Correctness x Recording Site: $F_{2,16} = 4.5$, $p = 0.03$) versus no effect in the control group ($F < 2.0$). Error minus correct difference maps at 390 ms are displayed in Fig. 5.

4. Discussion

4.1. Healthy participants' P3

S-locked and R-locked P3 amplitudes at Pz were equally large in healthy participants, as expected in hypothesis 1.a (cf. Section 1.5). This equality held both for fast responses, induced by compatible flankers, and for slow responses, induced by incompatible flankers, spanning a range of mean RTs from 475 ms to 605 ms. This confirms previous evidence on equality of S- and R-locked amplitudes across fast and slow RT quartiles (Poli et al., 2010; Verleger et al., 2005) and across fast- and slow-responding participants (Saville et al., 2011) and extends this evidence from young adults to elderly adults. Corresponding results, though not quantified, have also been shown in young adults in a flanker task very similar to the present one (Kopp et al., 1996; their Figs. 6 and 7). The present data also confirmed the utility of forming R- and S-locked averages for separating the P3 complex into two main constituents. Like in young adults (Verleger et al., 2005) the frontal part of the P3 complex, measured at Fz, was larger in S- than in R-locked data while the parietal part, measured at Pz, kept its amplitude equal in S- and R-locked data. This evidence lends itself to the interpretation (Gaeta, Friedman, & Hunt, 2003) that the frontal, S-locked part is P3a, akin to the orienting response and the parietal, S–R-integrating part is P3b, related to

stimulus relevance, i.e., to the information provided by the stimuli for taking some decision.

4.2. Reduction of PD patients' P3

We had assumed (hypothesis 1.b in Section 1.5), based on both Stocco et al.'s (2010) and Schroll et al.'s (in press) models, that PD patients' P3 would be reduced by a process related to their dysfunctional stimulus-induced response activation. Therefore, their R-locked P3 was compared to their S-locked P3 and indeed was found to be specifically reduced (left parts of Figs. 4-6), in contrast to healthy participants (right parts of Figs. 4-6). No difference was obtained between groups in the usual S-locked P3b amplitude, which agrees with several studies listed in the Introduction (Bokura et al., 2005; Low et al., 2002; Praamstra et al., 1996, 1998; Stemmer et al., 2007; Tachibana et al., 1992, 1997; Willemssen et al., 2011; Wright et al., 1997). Nor did the two groups differ in their R-locked amplitudes, in spite of the distinct and reliable reduction of R-locked vs. S-locked amplitudes in PD patients' intraindividual analysis. Thus, there was obviously large interindividual variance which precluded these reductions from inducing a group difference in the R-locked data.

Possible mechanisms underlying this response-related reduction, to be discussed in the following, refer to variability of response processing, compensation for dysfunctional response processing (cf. Stocco et al., 2010), and the presence of conflicting response tendencies (cf. Schroll et al., in press). As will be discussed, the reduction of R-locked P3b amplitudes was not due to reductions of the very P3b but due to a fronto-central negative shift, overlapping PD patients' P3b in the final 100 ms before overt responding. This negative shift may be related to compensatory cortical

movement preparation (Section 4.2.2) or, as hypothesized, may be an N-type negativity, indicating the presence of conflicting response tendencies (Section 4.2.3). In this context, the N_E results will be discussed, measured in trials with incorrect responses by R-locked averaging (Section 4.3). In particular, the fact that N_E was more prominent in PD patients than in the healthy group in S-locked averages when incorrectly responded trials were compared to correctly responded trials (Section 4.2.3) provides converging evidence for an altered balance between N-type negativities and P3b in PD patients.

4.2.1. Variability of response processing

According to recent theories and computational models (e.g., Stocco et al., 2010; Schroll et al., in press) PD patients lack a smooth transition from stimulus-processing to responding. Thus, the P3b process initiated by S processing may go astray and not properly culminate at the time of R. Therefore, when timing of P3b varies across trials more with respect to R than to S, R-locked P3b will be reduced. If so, the reduction should be largest where P3b is largest, at Pz. Yet, this was not the case. Rather, the reduction was largest at Cz, and still larger at Fz than at Pz. Moreover, this account in terms of RT variability implies that RTs are more variable across trials in PD patients than in healthy controls. But there was only a weak, non-significant tendency for such larger variability (Fig. 3). Not being due to increased variability and being largest at more anterior sites than at Pz, it appears that the reduction of R-locked P3b was due to some overlapping R-related negative process, maximum at Cz and Fz. Being R-related, this process would vary across time in S-locked averages and, therefore, affects P3b less in S- than R-locked averages.

4.2.2. Compensation for dysfunctional response processing

One such centrally focused R-related negativity is the Bereitschaftspotential (BP). BPs are usually measured in tasks without any S where participants have to repeatedly perform some movement at their own pace. Then, the first phase of BPs reflects the decision and timing for preparing the movement, and the second phase reflects immediate preparation of the movement. The first phase is mainly generated in mesial areas, above all the supplementary motor area, and the second phase is generated in the lateral motor cortex M1 contralateral to the responding hand (review: Shibasaki & Hallett, 2006). Even though minor alterations have been reported, BPs in such self-paced tasks are principally similar in PD patients and healthy persons (review: Verleger, 2012). In tasks like here where R is determined and triggered by the preceding S rather than being generated in a self-paced manner, portions of the second phase may be measured as "lateralized readiness potential" (cf. for the present data Verleger et al., 2010) whereas the first, mesially generated phase is absent in healthy persons (Baker, Piriyapunyaporn, & Cunnington, 2012; Waszak et al., 2005) which might be due to automatic routing between processing S and producing R (Stocco et al., 2010). When this routing is deficient, PD patients may need to produce this first part of the BP, implementing some compensatory strategy for basal ganglia malfunction by recruiting cortical areas for initiating R, in line with Stocco et al.'s (2010) model. This additional BP would be time-locked to R and thereby reduce the overlapping P3 in the R-locked average. In this interpretation, the reduction of R-locked P3 reflects a compensatory process needed by PD patients in order to respond according to instructions.

4.2.3. Presence of conflicting response tendencies

Alternatively, the centrally focused R-related negativity which overlaps and reduces R-locked P3 may be a conflict-related negativity of the N2b/N-type, not occurring after the response like N_E but rather before the response like "N-120", which was recently described in healthy young adults as a negativity preceding the correct response in high-conflict trials (Mansfield et al., 2012; Vidal et al., 2011). This negativity, culminating before the response, would reflect the increase of conflicting response tendencies as PD patients come closer to the response. This notion of permanent and increased ambiguity is a prediction made by Schroll et al.'s (in press) model of basal-ganglia functioning where a role is described for the basal ganglia in clearing conflicts between different S–R associations. In Schroll et al.'s (in press) simulations, PD is predicted to lead to increased response conflict when linking S to R, resulting in less reliable motor-cortical activation of the correct R and even in activation of incorrect Rs. This increased conflict might be reflected in the observed negativity. In this view, rather than indicating a compensatory process as would do the BP (Section 4.2.2) this negativity before the response reflects a core pathology of PD patients.

Converging evidence for the assumption of increased conflict in PD patients was obtained from their changed balance between N_E and P3 in incorrectly responded trials. The error negativity, N_E, could not only be seen in R-locked data, as in the healthy group, but also in PD patients' S-locked data, around 400 ms after the target, which roughly fits the 430 ms latency that was to be expected based on the mean RT of 370 ms in error trials and N_E's peak latencies of 60 ms after R. Inspection of the overlaid S- and R-locked averages in PD patients (Fig. 8) left few doubts that this negative component in the S-locked average is the same component as N_E in the R-

locked average, rather than some additional component like S-related N2 (Yeung et al., 2004) or R-related "N-120" (Mansfield et al., 2012; Vidal et al., 2011). This S-locked N_E was less distinct in healthy participants. In contrast, there was an early P3 complex in the healthy group, evoked by incorrectly responded stimuli, reaching its peak at about 300 ms after target onset. This is very early for P3 evoked by visual stimuli in elderly participants (van der Lubbe & Verleger, 2002; Zeef, Sonke, Kok, Buiten, & Kenemans, 1996). Therefore, this P3 was probably not evoked by the target but by the flankers that were presented 100ms before the target in this condition.

Accordingly, this distinct early P3 in healthy participants' incorrect responses probably reflects these participants' fast and unambiguous (though incorrect) choice for these incorrect responses erroneously triggered by the flankers. This P3 did not develop to the same extent in PD patients. Rather, their prevailing N_E appeared to reflect the permanent state of conflict in their response selection. This changed balance between N_E and P3 in PD patients' error trials provides support for the idea that something similar might occur in correct trials, as suggested in the preceding paragraph: the process that overlaps and reduces P3 in PD patients' correct trials might thus be a negativity that indicates the ongoing conflict of response tendencies as described by Schroll et al.'s (in press) model.

4.3. Limitations of this study

No reliable group differences in the R-locked N_E in error trials were obtained in the present study. This absence of a difference replicates Holroyd et al. (2002) but may be considered an unusual result in view of the number of studies that reported reliably smaller N_E in PD patients (Falkenstein et al., 2001; Ito & Kitagawa, 2006; Stemmer et al., 2007; Willemssen et al., 2008, 2009). Stemmer et al. (2007) note that

it was only at FCz where their group difference was significant, and this is also the only recording site reported by Falkenstein et al. (2001) and Willemssen et al. (2008, 2009). Correspondingly, the non-significant result reported by Holroyd et al. (2002) was reported in data from Cz and Fz only. Thus, the probable reason for the lacking effect in our data is that we had not recorded from FCz where N_E is usually largest. We were mistaken in not recording from FCz. We may assume that also our R-locked negativity before the response would have been largest at FCz. We may note that FCz recording would not have helped in distinguishing between error- or control-related negative components (Section 4.2.3) from Bereitschaftspotential-type components (Section 4.2.2) because also the latter is usually largest at FCz (e.g., Ball et al., 1999).

As has often been done in ERP studies on PD patients, PD patients were here tested in their best "on"-phase, i.e., under optimum medication. Therefore, it must principally remain unclear whether the group differences are due to effects of the disease, which include lack of dopamine in the basal ganglia, or, on the contrary, due to effects of medication. Moreover, it remains unclear, in how far optimum medication (which is determined separately for each patient based on their overt symptoms) results in (still) reduced dopamine levels or may involve some dopamine overshoot. The models' predictions as depicted in Fig. 1 hold true for reduced dopamine levels only; they do not generalize to dopamine overshoot. Presumably, there is no simple answer to the question of whether dopamine levels are reduced or increased: Different nuclei of the basal ganglia, and even different parts of these nuclei, suffer from different amounts of dopamine loss (Pavese, Rivero-Bosch, Lewis, Whone, & Brooks, 2011), while replacement is given at the systemic level and thus presumably targets all nuclei equivalently. Thus, some nuclei may experience reduced dopamine levels under optimum medication, while at the same time others may

experience overshoots. Since, however, motor regions of the basal ganglia are affected most severely (Pavese et al., 2011), it is likely that these still suffer from dopamine loss under optimum medication: A full restoration of dopamine levels in motor regions would likely cause severe overshoots and corresponding side-effects in cognitive and limbic domains of the basal ganglia. To empirically estimate the effects of medication, PD patients may be tested twice, once in the "on" phase and once in the "off" phase (usually after overnight withdrawal from medication). However, earlier studies, including our own (Vieregge, Verleger, Wascher, Stüven, & Kömpf, 1994) failed to find relevant effects between "on" and "off" states, and particularly failed so for P3 amplitude (Starkstein, Esteguy, Berthier, Garcia, & Leiguarda, 1989; Stemmer et al., 2007; Willemssen et al., 2011) and for N_E (Stemmer et al., 2007). Alternatively, possibly more sensitive to medication effects, newly diagnosed ("de novo") patients may be tested, once before they receive any medication and once some time later. This was done by Willemssen et al. (2011) but, again, no effects on P3 amplitudes were reported. Similarly, N_E was found to be reduced in de-novo PD patients (Willemssen et al., 2009).

It may be noted that Willemssen et al. (2011) reported a reduced positivity at 400–500 ms after S onset in de-novo patients' compatible trials compared to control participants. Willemssen et al. attributed this effect to the preceding (S-locked) N2 peak but actually the effect was close to the patients' average response times in this condition and might, therefore, rather reflect the R-locked negativity that we have described here. As judged from Willemssen et al.'s Fig. 1, also this effect remained stable in these patients after they had received medication.

To summarize, effects of medication or withdrawal of medication on PD patients' ERPs have been minor at best in the literature. Reasons for this are not clear.

But, by inference, we may assume that also the effects reported in the present study do not largely depend on medication.

4.4. Relevance for models of basal-ganglia function

PD patients' P3b component was reduced at central and frontal sites by an overlapping negative component that preceded the key-press response. This negative component probably reflects response conflict, similar to the error negativity (N_E). This suggests that PD patients experience increased cortical response conflicts in S-R tasks. Such conflicts are in line with Schroll et al.'s (in press) model according to which dysfunctional cortico-basalganglio-thalamic loops in PD suppress correct responses and facilitate incorrect responses.

It has been proposed previously that basal ganglia vitally participate in response selection, for instance by the computational models of Brown et al. (2004), Frank (2006), Ashby et al. (2007), Guthrie, Myers, and Gluck (2009) and Stocco et al. (2010). Of these, the models by Guthrie et al. (2009), Frank (2006) and Stocco et al. (2010) have been explicitly used to simulate the effects of dopamine loss on basal ganglia functioning. The predictions by Stocco et al.'s (2010) model have been extensively portrayed (Section 1.1) and related to our findings (Section 4.2.2). Both Frank's (2006) and Guthrie et al.'s (2009) simulations predict that extensive dopamine loss results in deficits to select correct responses, similar to the predictions by Schroll et al.'s (in press) and Stocco et al. (2010). However, their simulations neither predict that cortico-basalganglio-thalamic loops learn to actively suppress correct responses and to facilitate incorrect responses in Parkinsonian networks, resulting in increased response conflict (cf. Schroll et al., in press), nor that cortex compensates for basal ganglia dysfunction in PD (cf. Stocco et al., 2010). Therefore, their models might be

best in line with an increased cortical response uncertainty rather than with increased response conflict or with cortical compensation – but neither Frank (2006) nor Guthrie et al. (2009) explicitly predicted the consequences of dopamine loss on cortical processing. Our findings do not provide direct support for these theories: As outlined above (Section 4.2), we found an additional negative ERP component in PD patients that could be interpreted as a compensatory process (Section 4.2.2) or, more likely, as a conflict-related process (Section 4.2.3), but that does not likely reflect response uncertainty.

Increased response conflict seems to capture a major patho-physiological feature of PD: As a component of what has been called "dysexecutive syndrome", PD patients have often been described to have difficulties in clearly distinguishing and flexibly switching between alternatives (e.g., Brown & Marsden, 1990; Ceravolo, Pagni, Tognoni, & Bonuccelli, 2012; Cools, Rogers, Barker, & Robbins, 2010; Ravizza & Ivry, 2001; Williams-Gray et al., 2009). It remains to be shown whether the reduction of R-locked P3 is a direct measure of this dysexecutive syndrome.

Funding

The authors arranged their cooperation on this topic during a meeting funded by Deutsche Forschungsgemeinschaft for collaboration within the package proposal "neuro-cognitive mechanisms of conscious and unconscious visual perception" (PAK 270). FHH and HS were supported by HA 2630/6-1 (PAK 270); HS is additionally supported by HA 2630/7-1 (KFO 247).

Acknowledgments

Thanks are due to Johann Hagenah for clinical assessment of the participants and to Manuel Weiß for his help in EEG recording. The P3 part of these data was presented as a poster at ICON 12, the 12th International Conference on Cognitive Neuroscience, in Palma de Mallorca (Spain), September 25–29, 2011.

Tables

Table 1:

Patient	Age (years)	Sex	Disease Duration (years)	Hoehn and Yahr	UPDRS III	Medication (l-dopa equivalence, in mg/ day)
1	50	m	2	2	13	600
2	73	m	3	2.5	21	300
3	63	m	8	2.5	18	900
4	67	m	12	3	26	900
5	68	f	2	2	18	700
6	52	f	2	3	22	600
7	71	m	3	2	20	300
8	79	m	1	1	5	150
9	66	m	3	2	14	450
10	59	m	8	2	15	1050
11	62	m	2	2	40	150
12	69	f	3	1.5	20	150

Table 1: Characteristics of the PD patients.

Figure legends

Figure 1. Model predictions on S-R processing in cortex and basal ganglia under normal dopamine levels and under Parkinsonian dopamine loss. (A) The model by Stocco et al. (2010) predicts that dopamine loss results in reduced basal-ganglia activity and in increased cortical processing. (B) The model by Schroll et al. (in press) predicts that dopamine loss causes changes in the outputs of basal-ganglia and cortico-thalamic pathways that differentially affect correct motor programs (circle center) and incorrect motor programs (circle surrounds). Taken together, excitation of the correct motor program is reduced, while excitation of incorrect motor programs is increased, thus causing response conflicts.

Figure 2. Types of stimulus sequences in a trial, exemplified for left-pointing target stimuli. Target arrows pointed left or right in random order across trials. The temporal interval between flankers and targets was either 0 ms ("FTI 0") or 107 ms ("FTI 100") in random order across trials. The stimuli were black, the fixation cross was red. This scheme is from participants' point of view and of primary importance for the present purpose. Actually, the neutral flankers masked preceding briefly (13 ms) presented flankers (which were compatible or incompatible in random order).

Figure 3. Response-time statistics, means across participants. Upper half: mean RTs in ms relative to target onset. Lower half: standard deviation of RTs. "Comp." and "inc." (on x-axis) denote compatible and incompatible trials. FTI = flanker-target interval. Black lines mark PD patients, gray lines the healthy participants. The error bars denote 95% confidence intervals of interindividual variation (plotted on one side only, for better discriminability).

Figure 4. Grand means of ERPs in the neutral (masked) FTI 0 ms condition. Left side: patients with Parkinson's disease (bold lines). Right side: healthy participants (thin lines). The waveforms depict the potentials recorded at the three midline sites Fz, Cz, Pz, as well as recordings of the vertical EOG (to evaluate possible ocular artifacts in the EEG). Negative voltage is drawn upwards. Tick marks at y-axis denote 2.5 mV for EEG and 50 mV for EOG. S-locked averages are in red, R-locked averages in blue. 0 ms on the red x-axis denotes target onset. R-locked averages and their time-axis (blue) were shifted backward by 48 ms such that R- and S-locked waveforms had most overlap (cf. Section 2.5). (For interpretation of the references to color in this figure legend, the reader is referred to the web version of this article.)

Figure 5. Maps of topographical distributions of differences between data displayed in Figs. 4, 8, 7, 9 (from top to bottom). In the R-locked minus S-locked maps (top two rows) blue indicates more negativity in the R-locked average, red more negativity in the S-locked average. In the error minus correct maps (bottom two rows) black indicates more negativity in error trials, white more negativity in correct trials. Time points of maps are the grand-mean peaks of S-locked P3 in the top row, of R-locked N_E in the two middle rows, and of patients' S-locked N_E (390 ms) in the bottom row. (For interpretation of the references to color in this figure legend, the reader is referred to the web version of this article.)

Figure 6. Grand means of ERPs recorded from Cz showing the PD patients' difference between R-locked and S-locked P3 in each of the six combinations of three flanker types and two flanker–target lags. Left side: patients with Parkinson's disease

(bold lines). Right side: healthy participants (thin lines). Negative voltage is drawn upwards. Tick marks at y-axis denote 2.5 mV. S-locked averages are in red, R-locked averages in blue. 0 ms on the red x-axis denotes target onset. R-locked averages were shifted backward by 48 ms, which produced best overlap with the red waveform in most conditions (cf. Section 2.5). The blue R-locked x-axis denotes the time scale of the neutral (masked) FTI 0 ms condition. (For interpretation of the references to color in this figure legend, the reader is referred to the web version of this article.)

Figure 7. Grand means of R-locked ERPs in error and correct-response trials in the FTI 100 ms condition, from n = 9 participants in either group. Left side: patients with Parkinson's disease (bold lines). Right side: healthy participants (thin lines). The waveforms depict the potentials recorded at the three midline sites Fz, Cz, Pz, as well as recordings of the vertical EOG (to evaluate possible ocular artifacts in the EEG). Negative voltage is drawn upwards. Tick marks at y-axis denote 2.5 mV for EEG and 50 mV for EOG. Error-trial averages are in black, correct-trial averages are in gray. 0ms on the x-axis denotes time of the keypress. The brief dashed horizontal lines denote pre-stimulus baseline levels.

Figure 8. Grand means of ERPs in error trials of the FTI 100 ms condition, from n = 9 participants in either group. Same format as Fig. 4. Like in Fig. 4, time-point zero of the blue x-axis is 48 ms earlier than the mean error-RT, which was 372 ms (cf. Section 2.5).

Figure 9. Grand means of S-locked ERPs in error and correct-response trials in the FTI 100 ms condition, from n = 9 participants in either group. Same format as Fig. 7,

though S- rather than R-locked. The shaded areas denote the two 50 ms epochs where the Correctness x Group and Correctness x Recording Site x Group effects were significant.

References

Ashby, F. G., Ennis, J. M., & Spiering, B. J. (2007). A neurobiological theory of automaticity in perceptual categorization. *Psychological Review*, *114*, 632–656.

Baker, K. S., Piriyapunyaporn, T., & Cunnington, R. (2012). Neural activity in readiness for incidental and explicitly timed actions. *Neuropsychologia*, *50*, 715–722.

Ball, T., Schreiber, A., Feige, B., Wagner, M., Lücking, C. H., & Kristeva-Feige, R. (1999). The role of higher-order motor areas in voluntary movement as revealed by high-resolution EEG and fMRI. *NeuroImage*, *10*, 682–694.

Beste, C., Dziobek, I., Hielscher, H., Willemssen, R., & Falkenstein, M. (2009). Effects of stimulus-response compatibility on inhibitory processes in Parkinson's disease. *European Journal of Neuroscience*, *29*, 855–860.

Birbaumer, N., Elbert, T., Canavan, A. G. M., & Rockstroh, B. (1990). Slow potentials of the cerebral cortex and behavior. *Physiological Reviews*, *70*, 1–41.

Bokura, H., Yamaguchi, S., & Kobayashi, S. (2005). Event-related potentials for response inhibition in Parkinson's disease. *Neuropsychologia*, *43*, 967–975.

Brooks, D. J. (2006). Dopaminergic action beyond its effects on motor function: imaging studies. *Journal of Neurology*, *253*(Suppl. 4), SIV8–SIV15.

Brown, J. W., Bullock, D., & Grossberg, S. (2004). How laminar frontal cortex and basal ganglia circuits interact to control planned and reactive saccades. *Neural Networks*, *17*, 471–510.

Brown, R. G., & Marsden, C. D. (1990). Cognitive function in Parkinson's disease: from description to theory. *Trends in Neurosciences*, *13*, 21–29.

Cavanagh, J. E., Zambrano-Vazquez, L., & Allen, J. J. B. (2012). Theta lingua franca: A common mid-frontal substrate for action monitoring processes. *Psychophysiology*, *49*, 220–239.

Ceravolo, R., Pagni, C., Tognoni, G., & Bonuccelli, U. (2012). The epidemiology and clinical manifestations of dysexecutive syndrome in Parkinson's disease. *Frontiers in Neurology*, *3*, 159, http://dx.doi.org/10.3389/fneur.2012.00159.

Cools, R., Rogers, R., Barker, R. A., & Robbins, T. W. (2010). Top-down attentional control in Parkinson's disease: Salient considerations. *Journal of Cognitive Neuroscience*, *22*, 848–859.

Debener, S., Ullsperger, M., Siegel, M., Fiehler, K., von Cramon, D. Y., & Engel, A. K. (2005). Trial-by-trial coupling of concurrent electroencephalogram and functional magnetic resonance imaging identifies the dynamics of performance monitoring. *Journal of Neuroscience*, *25*, 11730–11737.

Fahn, S., & Elton, R. L. (1987). members of the UPDRS development committee. (1987). Unified Parkinsons Disease Rating Scale. In: S. Fahn, C. D. Marsden, D. B. Calne, & M. Goldstein (Eds.), *Recent developments in Parkinson's disease*, vol. 2 (pp. 153–163). Florham Park, NJ: Macmillan Healthcare Information.

Falkenstein, M., Hohnsbein, J., Hoormann, J., & Blanke, L. (1991). Effects of cross-modal divided attention on late ERP components. II. Error processing in choice reaction tasks. *Electroencephalography and Clinical Neurophysiology*, *78*, 447–455.

Falkenstein, M., Hielscher, H., Dziobek, I., Schwarzenau, P., Hoormann, J., Sundermann, B., et al. (2001). Action monitoring, error detection, and the basal ganglia: an ERP study. *NeuroReport*, *12*, 157–161.

Fogelson, N., Fernandez-del-Olmo, M., & Santos-Garcia, D. (2011). Contextual processing deficits in Parkinson's disease: The role of the frontostriatal system. *Clinical Neurophysiology*, *122*, 539–545.

Folstein, J. R., & van Petten, C. (2008). Influence of cognitive control and mismatch on the N2 component of the ERP: A review. *Psychophysiology*, *45*, 152–170.

Frank, M. J. (2006). Hold your horses: a dynamic computational role for the subthalamic nucleus in decision making. *Neural Networks*, *19*, 1120–1136.

Gaeta, H.,Friedman, D., & Hunt, G. (2003). Stimulus characteristics and task category dissociate the anterior and posterior aspects of novelty P3. *Psychophysiology*, *40*, 198–208.

Gerson, A. D., Parra, L. C., & Sajda, P. (2005). Cortical origins of response time variability during rapid discrimination of visual objects. *NeuroImage*, *28*, 342–353.

Goetz, C. G., Poewe, W., Rascol, O., Sampaio, C., Stebbins, G. T., Counsell, C., et al. (2004). Movement disorder society task force report on the Hoehn and Yahr staging scale: Status and recommendations. *Movement Disorders*, *19*, 1020–1028.

Guthrie, M., Myers, C. E., & Gluck, M. A. (2009). A neurocomputational model of tonic and phasic dopamine in action selection: A comparison with cognitive deficits in Parkinson's disease. *Behavioural Brain Research*, *200*, 48–59.

Haber, S. N. (2003). The primate basal ganglia: parallel and integrative networks. *Journal of Chemical Neuroanatomy*, *26*, 317–330.

Hollerman, J. R., & Schultz, W. (2003). Dopamine neurons report an error in the temporal prediction of reward during learning. *Nature Neuroscience*, *1*,

304–309.

Holroyd, C. B., & Coles, M. G. H. (2002). The neural basis of human error processing: Reinforcement learning, dopamine, and the error-related negativity. *Psychological Review*, *109*, 679–709.

Holroyd, C. B., Praamstra, P., Plat, E., & Coles, M. G. H. (2002). Spared error-related potentials in mild to moderate Parkinson's disease. *Neuropsychologia*, *40*, 2116–2124.

Humphries, M. D., Stewart, R. D., & Gurney, K. N. (2006). A physiologically plausible model of action selection and oscillatory activity in the basal ganglia. *Journal of Neuroscience*, *26*, 12921–12942.

Ito, J., & Kitagawa, J. (2006). Performance monitoring and error processing during a lexical decision task in patients with Parkinson's disease. *Journal of Geriatric Psychiatry and Neurology*, *19*, 46–54.

Kopp, B., Rist, F., & Mattler, U. (1996). N200 in the flanker task as a neurobehavioral tool for investigating executive control. *Psychophysiology*, *33*, 282–294.

Low, K. A., Miller, J., & Vierck, E. (2002). Response slowing in Parkinson's disease. A psychophysiological analysis of premotor and motor processes. *Brain*, *125*, 1980–1994.

Lutzenberger, W., Elbert, T., & Rockstroh, B. (1987). A brief tutorial on the implications of volume conduction for the interpretation of the EEG. *Journal of Psychophysiology*, *1*, 81–89.

Maier, M. E., di Pellegrino, G., & Steinhauser, M. (2012). Enhanced error-related negativity on flanker errors: Error expectancy or error significance? *Psychophysiology*, *49*, 899–908.

Mansfield, K. L., van der Molen, M. W., & van Boxtel, G. J. M. (2012). Proactive and reactive control in S–R- compatibility: A brain potential analysis. *Psychophysiology*, *49*, 756–769.

Nambu, A., Tokuno, H., & Takada, M. (2002). Functional significance of the cortico-subthalamo-pallidal 'hyperdirect' pathway. *Neuroscience Research*, *43*, 111–117.

O'Connell, R. G., Dockree, P. M., & Kelly, S. P. (2012). A supramodal accumulation-to- bound signal that determines perceptual decisions in humans. *Nature Neuroscience*, *15*, 1729–1735.

Oldfield, R. C. (1971). The assessment and analysis of handedness: The Edinburgh Inventory. *Neuropsychologia*, *9*, 97–113.

Ouyang, G., Herzmann, G., Zhou, C., & Sommer, W. (2011). Residue Iteration Decomposition (RIDE): a new method to separate ERP components on the basis of latency variability in single trials. *Psychophysiology*, *48*, 1631–1647.

Ouyang, G., Schacht, A., Zhou, C., & Sommer, W. (2013). Overcoming limitations of the ERP method with Residue Iteration Decomposition (RIDE): A demonstration in go/no-go experiments. *Psychophysiology*, *50*, 253–265.

Pavese, N., Rivero-Bosch, M., Lewis, S. J., Whone, A. L., & Brooks, D. J. (2011). Progression of monoaminergic dysfunction in Parkinson's disease: A longitudinal F-dopa PET study. *NeuroImage*, *56*, 1463–1468.

Poli, R., Cinel, C., Citi, L., & Sepulveda, F. (2010). Reaction-time binning: A simple method for increasing the resolving power of ERP averages. *Psychophysiology*, *47*, 467–485.

Polich, J. (2007). Updating P300: An integrative theory of P3a and P3b. *Clinical Neurophysiology*, *118*, 2128–2148.

Praamstra, P., & Plat, F. M. (2001). Failed suppression of direct visuomotor activation in Parkinson's disease. *Journal of Cognitive Neuroscience*, *13*, 31–43.

Praamstra, P., Meyer, A. S., Cools, A. R., Horstink, M. W. I. M., & Stegeman, D. F. (1996). Movement preparation in Parkinson's disease: Time course and distribution of movement-related potentials in a movement precueing task. *Brain*, *119*, 1689–1704.

Praamstra, P., Stegeman, D. F., Cools, A. R., & Horstink, M. W. I. M. (1998). Reliance on external cues for movement initiation in Parkinson's disease: Evidence from movement-related potentials. *Brain*, *121*, 167–177.

Pulvermüller, F., Lutzenberger, W., Müller, V., Mohr, B., Dichgans, J., & Birbaumer, N. (1996). P3 and contingent negative variation in Parkinson's disease. *Electroencephalography and Clinical Neurophysiology*, *98*, 456–467.

Race, E. A., Badre, D., & Wagner, A. D. (2010). Multiple forms of learning yield temporally distinct electrophysiological repetition effects. *Cerebral Cortex*, *20*, 1726–1738.

Ravizza, S. M., & Ivry, R. B. (2001). Comparison of the basal ganglia and cerebellum in shifting attention. *Journal of Cognitive Neuroscience*, *13*, 285–297.

Ridderinkhof, K. R., Ullsperger, M., Crone, E. A., & Nieuwenhuis, S. (2004). The role of the medial frontal cortex in cognitive control. *Science*, *306*, 443–447.

Rodriguez-Oroz, M. C., Jahanshahi, M., Krack, P., Litvan, I., Macias, R., Bezard, E., et al. (2009). Initial clinical manifestations of Parkinson's disease: features and pathophysiological mechanisms. *Lancet Neurology*, *8*, 1128–1139.

Roman, R., Brázdil, M., Jurák, P., Rektor, I., & Kukleta, M. (2005). Intracerebral P3-like waveforms and the length of the stimulus-response interval in a visual oddball paradigm. *Clinical Neurophysiology*, *116*, 160–171.

Saville, C. W. N., Dean, R. O., Daley, D., Intrilligator, J., Boehm, S., Feige, B., et al. (2011). Electrocortical correlates of intra-subject variability in reaction times: Average and single-trial analyses. *Biological Psychology*, *87*, 74–83.

Schmiedt-Fehr, C., Schwendemann, G., Herrmann, M., & Başar-Eroğlu, C. (2007). Parkinson's disease and age-related alterations in brain oscillations during a Simon task. *NeuroReport*, *18*, 277–281.

Schroll, H., Vitay, J., & Hamker, F. H. (2012). Working memory and response selection: A computational account of interactions among cortico- basalganglio-thalamic loops. *Neural Networks*, *26*, 59–74.

Schroll, H., Vitay, J., Hamker, F.H. Dysfunctional and compensatory plasticity in Parkinson's disease. *European Journal of Neuroscience*, in press.

Seiss, E., & Praamstra, P. (2004). The basal ganglia and inhibitory mechanisms in response selection: evidence from subliminal priming of motor responses in Parkinson's disease. *Brain*, *127*, 330–339.

Seiss, E., & Praamstra, P. (2006). Time-course of masked response priming and inhibition in Parkinson's disease. *Neuropsychologia*, *44*, 869–875.

Shibasaki, H., & Hallett, M. (2006). What is the Bereitschaftspotential? *Clinical Neurophysiology*, *117*, 2341–2356.

Squires, N. K., Squires, K. C., & Hillyard, S. A. (1975). Two varieties of long-latency positive waves evoked by unpredictable auditory stimuli in man. *Electroencephalography and Clinical Neurophysiology*, *38*, 387–401.

Starkstein, S. E., Esteguy, M., Berthier, M. L., Garcia, H., & Leiguarda, R. (1989). Evoked potentials, reaction time and cognitive performance in on and off phases of Parkinson's disease. *Journal of Neurology, Neurosurgery, and Psychiatry*, *52*, 338–340.

Stemmer, B., Segalowitz, S. J., Dywan, J., Panisset, M., & Melmed, C. (2007). The error negativity in nonmedicated and medicated patients with Parkinson's disease. *Clinical Neurophysiology*, *118*, 1223–1229.

Stocco, A., Lebiere, C., & Anderson, J. R. (2010). Conditional routing of information to the cortex: a model of the basal ganglia's role in cognitive coordination. *Psychological Review*, *117*, 541–574.

Tachibana, H., Toda, K., & Sugita, M. (1992). Actively and passively evoked P3 latency of event-related potentials in Parkinson's disease. *Journal of the Neurological Sciences*, *111*, 134–142.

Tachibana, H., Aragane, K., Kawabata, K., & Sugita, M. (1997). P3 latency change in aging and Parkinson disease. *Archives of Neurology*, *54*, 296–302.

Takeda, Y., Sato, M., Yamanaka, K., Nozaki, D., & Yamamoto, Y. (2010). A generalized method to estimate waveforms common across trials from EEGs. *NeuroImage*, *51*, 629–641.

van der Lubbe, R. H. J., & Verleger, R. (2002). Aging and the Simon task. *Psychophysiology*, *39*, 100–110.

Verleger, R. (1988). Event-related potentials and cognition: A critique of the context updating hypothesis and an alternative interpretation of P3. *Behavioral and Brain Sciences*, *11*, 343–356.

Verleger, R. (2012). Alterations of ERP components in neurodegenerative diseases. In: S. J. Luck, & E. S. Kappenman (Eds.), *The Oxford handbook of event-related potential components* (pp. 593–610). New York: Oxford University Press.

Verleger, R., Jaśkowski, P., & Wascher, E. (2005). Evidence for an integrative role of P3b in linking reaction to perception. *Journal of Psychophysiology*, *19*, 165–181.

Verleger, R., Hagenah, J., Weiß, M., Ewers, T., Heberlein, I., Pramstaller, P., et al. (2010). Responsiveness to distracting stimuli, though increased in Parkinson's disease, is decreased in asymptomatic PINK1 and Parkin mutation carriers. *Neuropsychologia*, *48*, 467–476.

Vidal, F., Burle, B., Bonnet, M., Grapperon, J., & Hasbroucq, T. (2003). Error negativity on correct trials: a reexamination of available data. *Biological Psychology*, *64*, 265–282.

Vidal, F., Burle, B., Grapperon, J., & Hasbroucq, T. (2011). An ERP study of cognitive architecture and the insertion of mental processes: Donders revisited. *Psychophysiology*, *48*, 1242–1251.

Vieregge, P., Verleger, R., Wascher, E., Stüven, F., & Kömpf, D. (1994). Selective attention is impaired in Parkinson's disease—Event-related evidence from EEG potentials. *Cognitive Brain Research*, *2*, 117–130.

Waszak, F., Wascher, E., Keller, P., Koch, I., Aschersleben, G., Rosenbaum, D. A., et al. (2005). Intention-based and stimulus-based mechanisms in action selection. *Experimental Brain Research*, *162*, 346–356.

Willemssen, R., Müller, T., Schwarz, M., Hohnsbein, J., & Falkenstein, M. (2008). Error processing in patients with Parkinson's disease: the influence of medication state. *Journal of Neural Transmission*, *115*, 461–468.

Willemssen, R., Müller, T., Schwarz, M., Falkenstein, M., & Beste, C. (2009). Response monitoring in de novo patients with Parkinson's disease. *PLoS One*, *4*(3), e4898. Willemssen, R., Falkenstein, M., Schwarz, M., Müller, T., & Beste, C. (2011). Effects of aging, Parkinson's disease, and dopamnergic medication on response selection and control. *Neurobiology of Aging*, *32*, 327–335.

Williams-Gray, C. H., Evans, J. R., Goris, A., Foltynie, T., Ban, M., Robbins, T. W., et al. (2009). The distinct cognitive syndromes of Parkinson's disease: 5 year follow-up of the CamPaIGN cohort. *Brain*, *132*, 2958–2969.

Wright, M. J., Geffen, G. M., & Geffen, L. B. (1993). Event-related potentials associated with covert orientation of visual attention in Parkinson's disease. *Neuropsychologia*, *31*, 1283–1297.

Wylie, S. A., van den Wildenberg, W. P. M., Ridderinkhof, K. R., Bashore, T. R., Powell, V. D., Manning, C. A., et al. (2009). The effect of Parkinson's disease on interference control during action selection. *Neuropsychologia*, *47*, 145–157.

Yeung, N., Botvinick, M. M., & Cohen, J. D. (2004). The neural basis of error detection: Conflict monitoring and the error-related negativity. *Psychological Review*, *111*, 931–959.

Yordanova, J., Falkenstein, M., Hohnsbein, J., & Kolev, V. (2004). Parallel systems of error processing in the brain. *NeuroImage*, *22*, 590–602.

Zeef, E. J., Sonke, C. J., Kok, A., Buiten, M. M., & Kenemans, L. J. (1996). Perceptual factors affecting age-related differences in focused attention: Performance and psychophysiological analyses. *Psychophysiology*, *33*, 555–565.

Figures

Figure 1

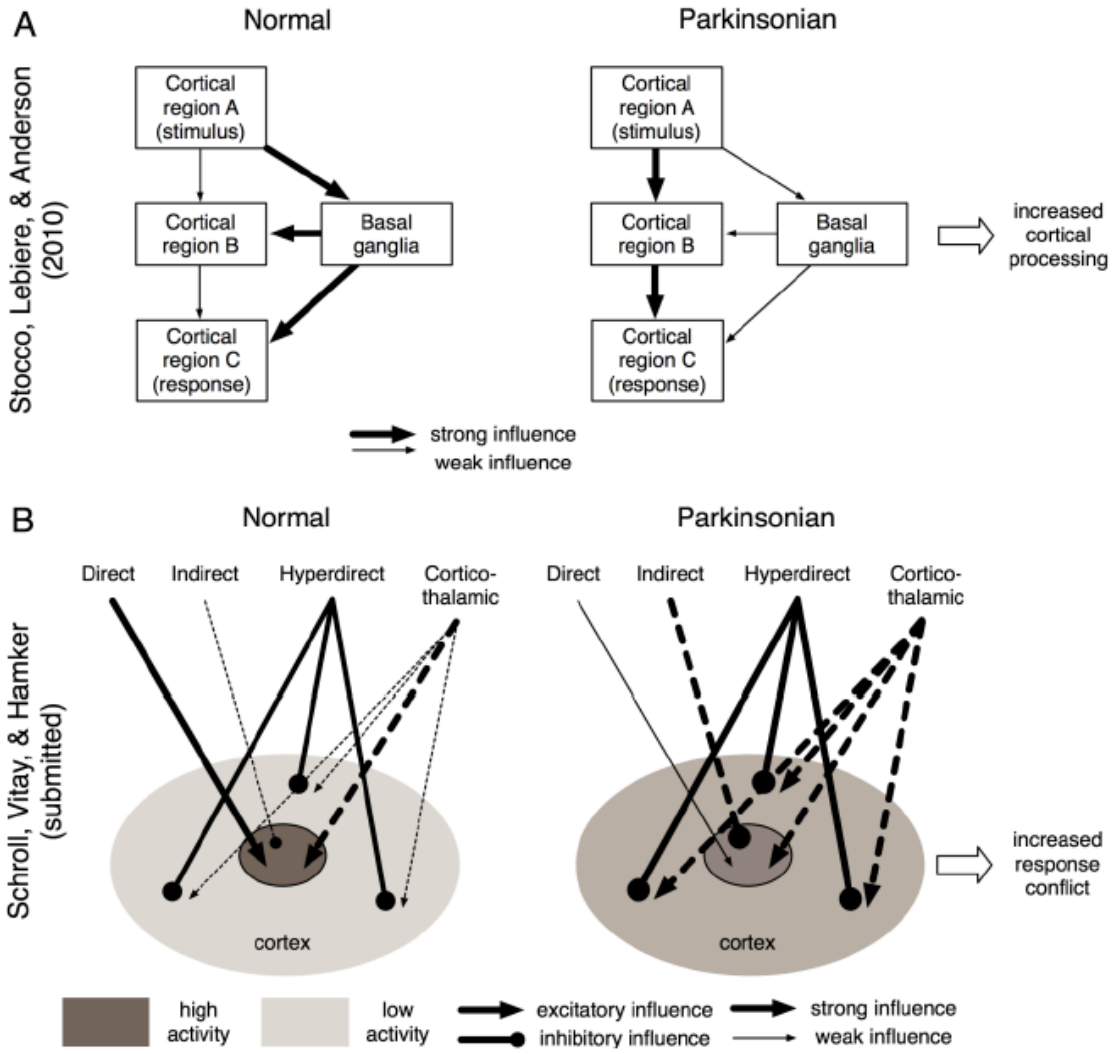

Figure 2

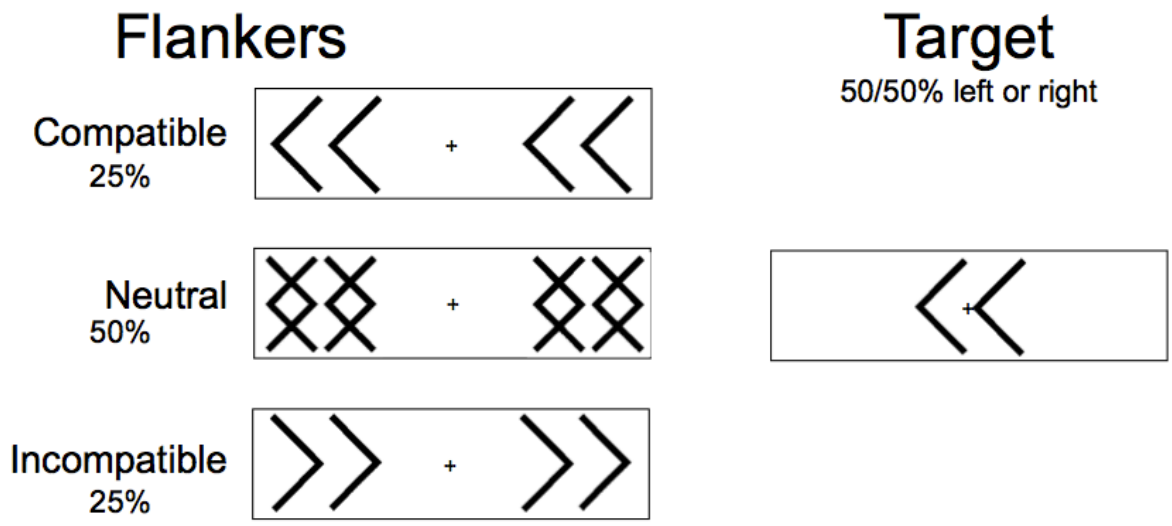
Flankers
Target
50/50% left or right
Compatible
25%
Neutral
50%
Incompatible
25%

Figure 3

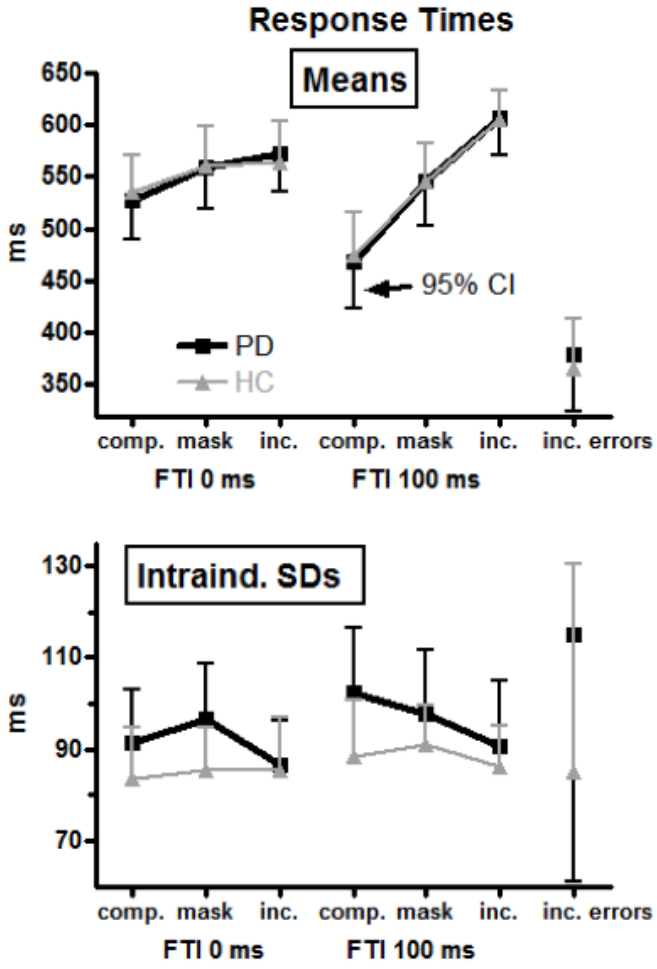
Response Times
Means
650
600
550
500
450
400
350
ms
95% CI
PD
HC
comp. mask inc. comp. mask inc. inc. errors
FTI 0 ms
FTI 100 ms
Intraind. SDs
130
110
90
70
ms
comp. mask inc. comp. mask inc. inc. errors
FTI 0 ms
FTI 100 ms

Figure 4

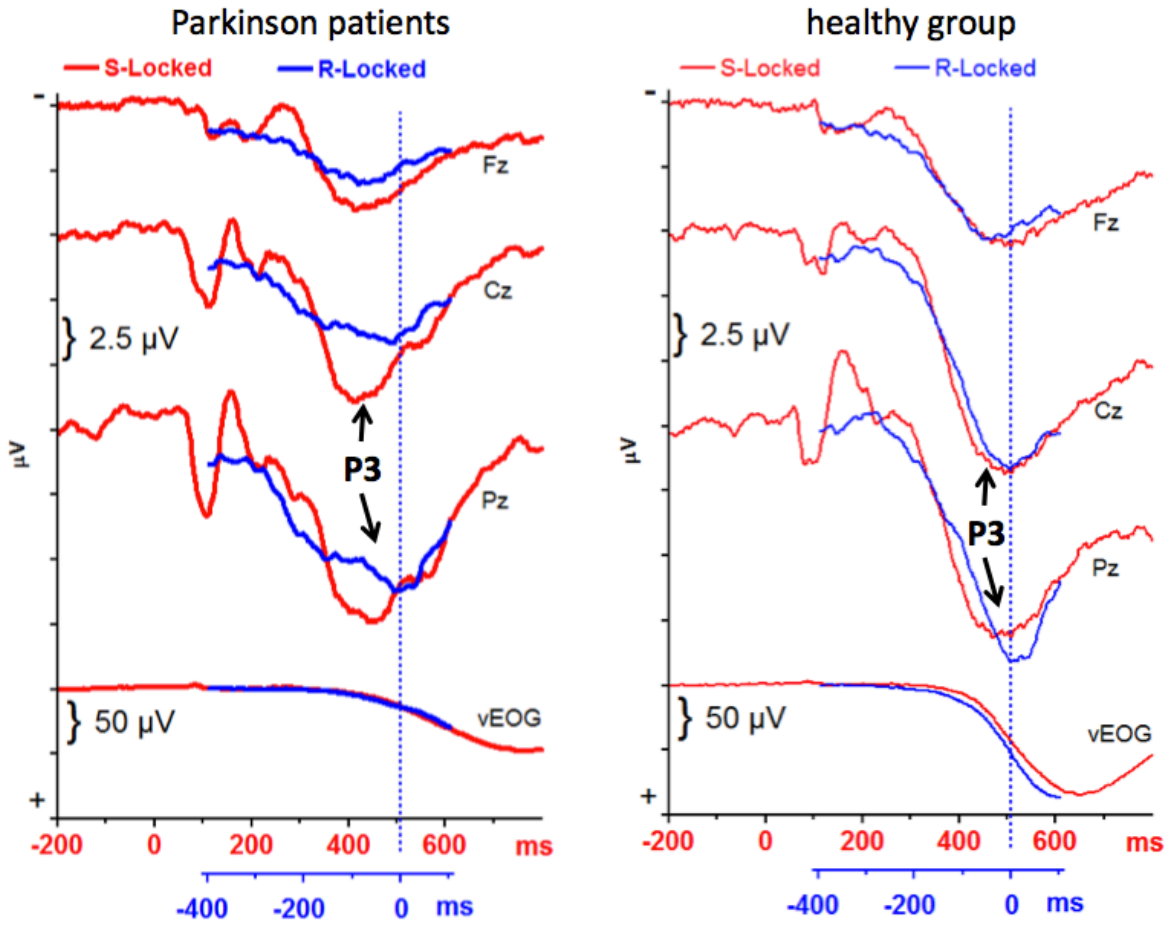
Parkinson patients
S-Locked
R-Locked
Fz
Cz
Pz
vEOG
2.5 µV
50 µV
P3
µV
-200
0
200
400
600
ms
-400
-200
0
ms
healthy group
S-Locked
R-Locked
Fz
Cz
Pz
vEOG
2.5 µV
50 µV
P3
µV
-200
0
200
400
600
ms
-400
-200
0
ms

Figure 5

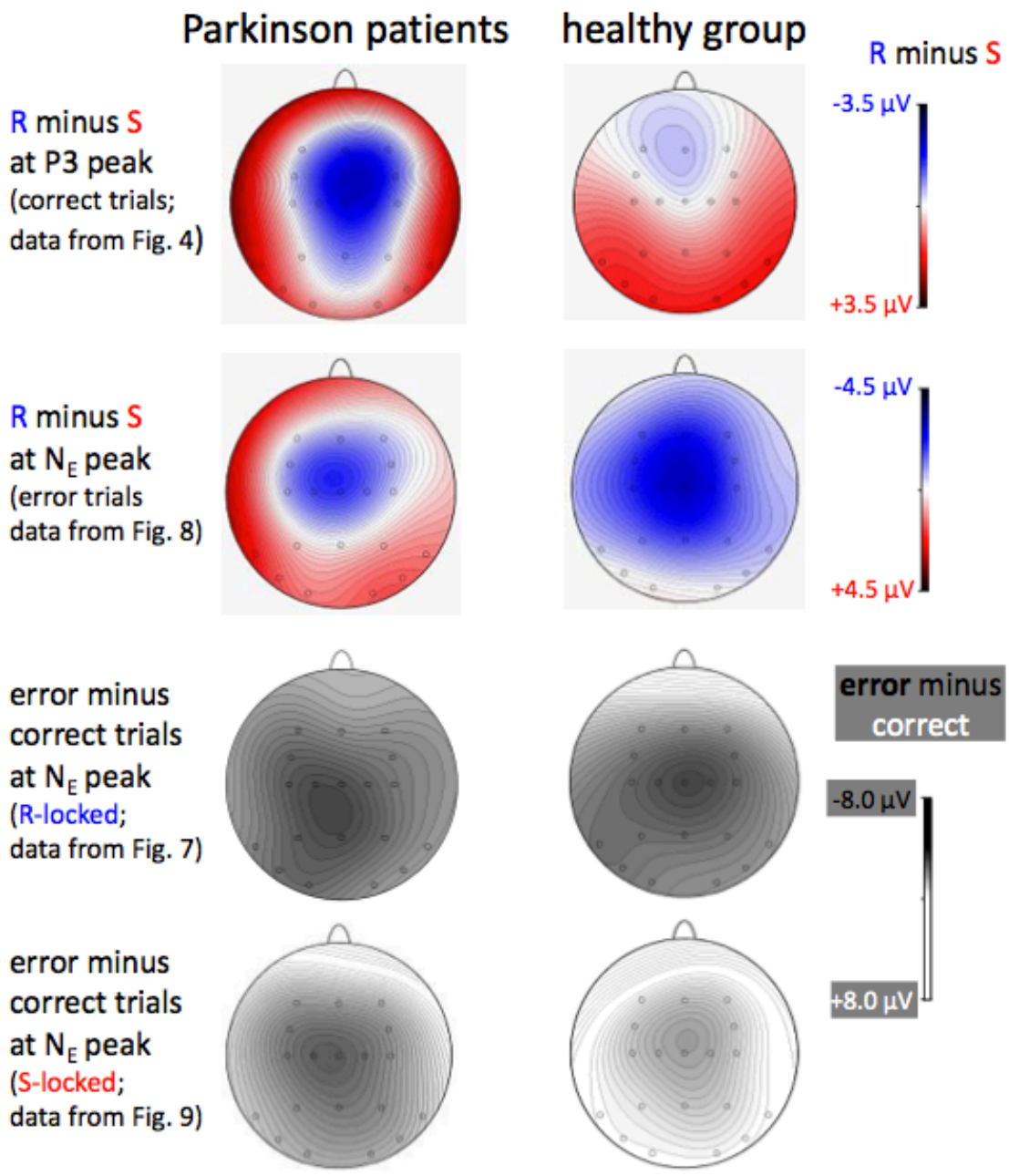
Parkinson patients
healthy group
R minus S
R minus S
at P3 peak
(correct trials;
data from Fig. 4)
-3.5 µV
+3.5 µV
R minus S
at N$_E$ peak
(error trials
data from Fig. 8)
-4.5 µV
+4.5 µV
error minus
correct trials
at N$_E$ peak
(R-locked;
data from Fig. 7)
error minus
correct
-8.0 µV
error minus
correct trials
at N$_E$ peak
(S-locked;
data from Fig. 9)
+8.0 µV

Figure 6

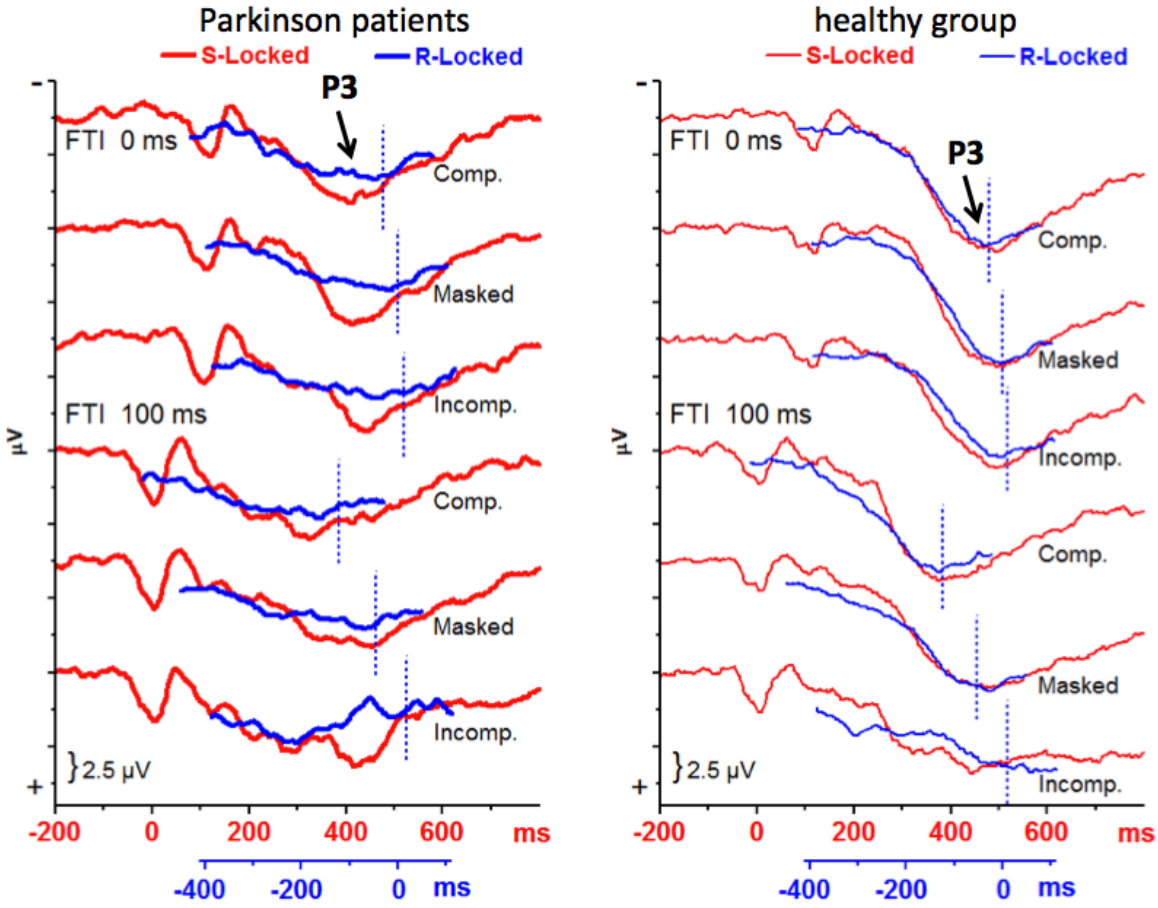
Parkinson patients
S-Locked
R-Locked
P3
FTI 0 ms
Comp.
Masked
Incomp.
FTI 100 ms
Comp.
Masked
Incomp.
2.5 µV
µV
-200
0
200
400
600
ms
-400
-200
0
ms
healthy group
S-Locked
R-Locked
FTI 0 ms
P3
Comp.
Masked
Incomp.
FTI 100 ms
Comp.
Masked
Incomp.
2.5 µV
µV
-200
0
200
400
600
ms
-400
-200
0
ms

Figure 7

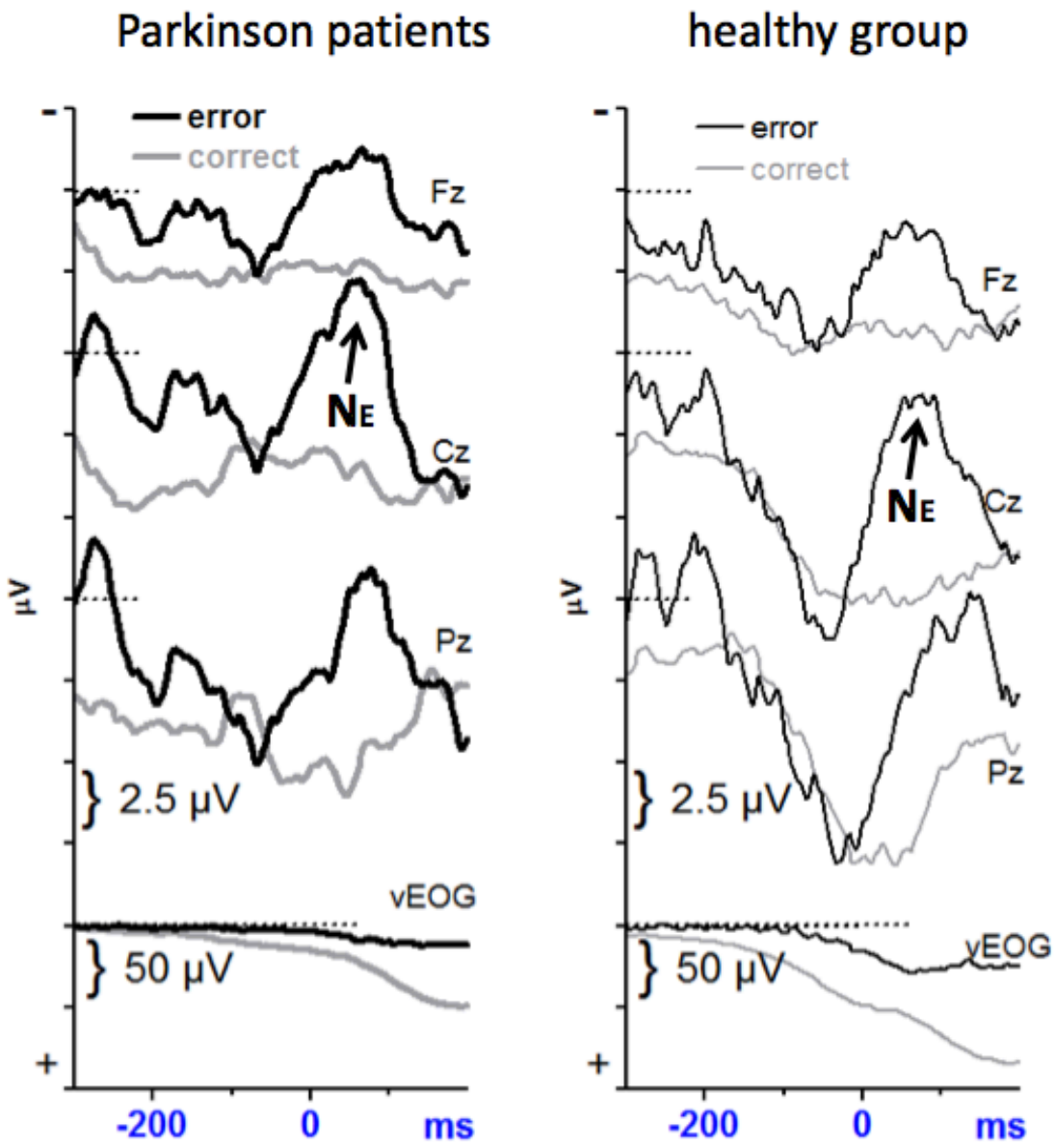
Parkinson patients
healthy group
error
correct
Fz
Cz
Pz
NE
μV
2.5 μV
vEOG
50 μV
-
+
-200
0
ms

Figure 8

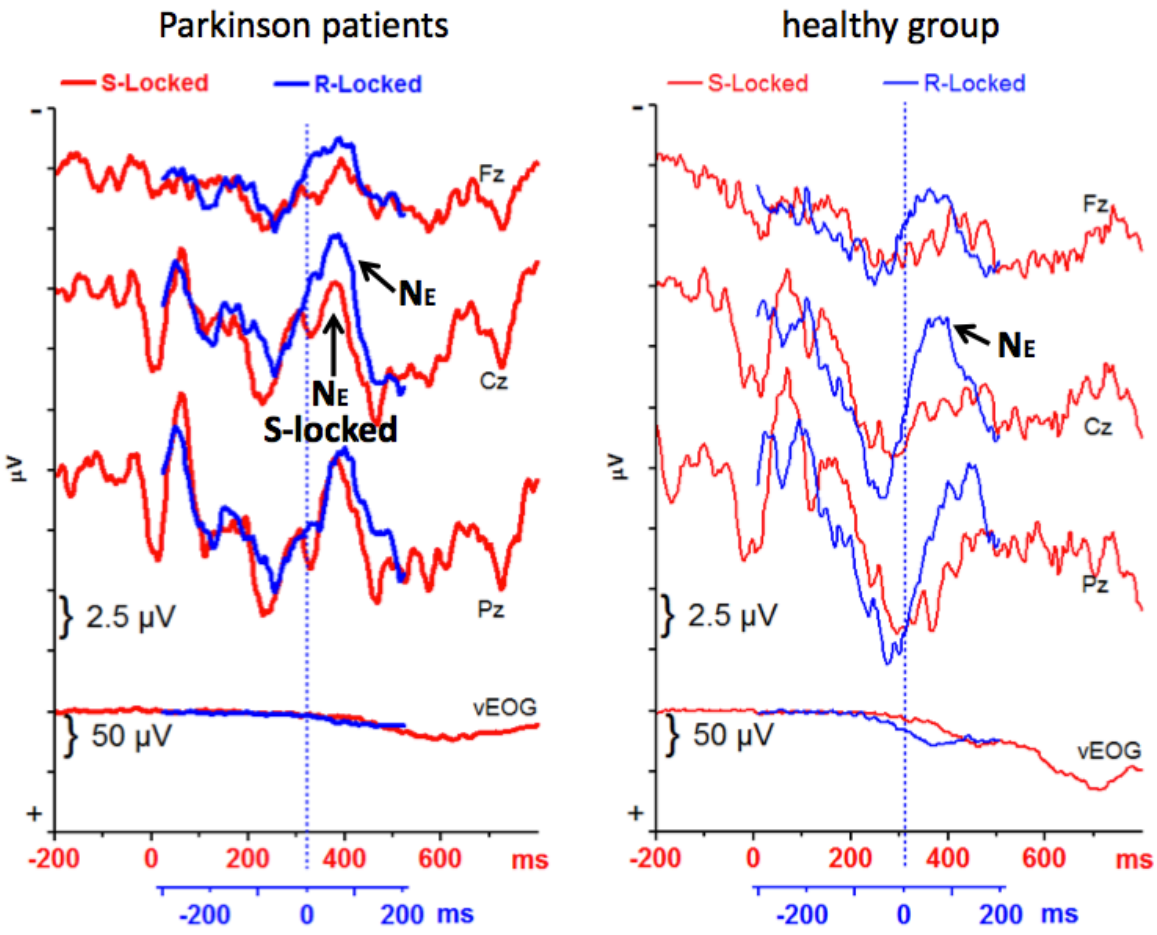
Parkinson patients
S-Locked
R-Locked
Fz
Cz
Pz
vEOG
NE
NE
S-locked
2.5 µV
50 µV
µV
-200
0
200
400
600
ms
-200
0
200 ms
healthy group
S-Locked
R-Locked
Fz
Cz
Pz
vEOG
NE
2.5 µV
50 µV
µV
-200
0
200
400
600
ms
-200
0
200 ms

Figure 9

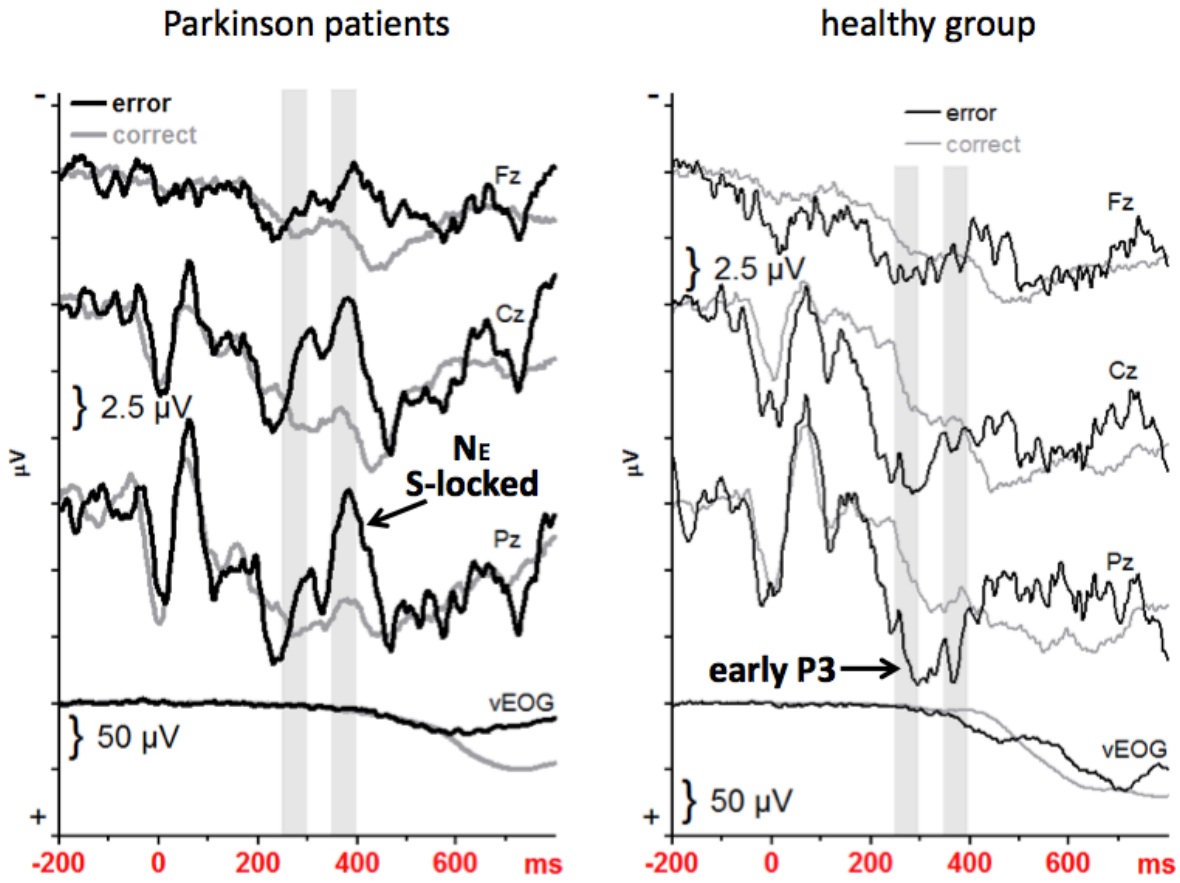
Parkinson patients
healthy group
error
correct
Fz
Cz
Pz
vEOG
2.5 µV
50 µV
µV
NE
S-locked
early P3
-200
0
200
400
600
ms